Deanship of Graduate Studies

Al-Quds University

O^+ and H^+ ions outflow in the cusp and central polar cap regions

Ghadeer Yahya Mahmoud AL- Sarsour

M.Sc. Thesis

Jerusalem –Palestine

1436AH/2015AD

O^+ and H^+ ions outflow in the cusp and central polar cap regions

Prepared by :

Ghadeer Yahya Mahmoud AL- Sarsour

B.Sc. Physics (Al-Quds university) (Palestine)

Supervisor: **Prof. Dr. Imad A. Barghouthi**

A thesis Submitted in Partial Fulfillment of Requirement for the Degree of Master of Science in Department/physics Master

Faculty of Science / Al-Quds university

1436AH/2015AD

AL- Quds University

Deanship of Graduate Studies

M.Sc. Physics / Physics Department

Thesis Approval

O^+ and H^+ ions outflow in the cusp and central polar cap regions

Prepared by: Ghadeer Yahya Mahmoud AL- Sarsour

Registration No: 21020313

Supervisor: Prof. Dr. Imad A. Barghouthi

Master thesis submitted and accepted, Date: 6 / 6 / 2015

The names and signatures of the examining committee members are as follows:

1- Head of committee: Prof: Imad A. Barghouthi Signature …….
2- Internal Examiner: Dr. Husain ALsamamra Signature …….
3- External Examiner: Dr.lilia A.Mashal Signature …….

Jerusalem –Palestine

1436/2015

Dedication

To …..…….. The spirit of my dear father. (God's mercy From God to granted prestige and dignity, who taught me to tender without waiting, to carry the name proudly.

To…… The meaning of love and the meaning of compassion and dedication, to smile and walk of life to the presence of her du'aa as if the secret of my success and affection surgical balm , my beloved mother.

To …… from supported me and helped me in the way of my studies, patient dear to my husband

To ……... Of Sirte for her in the driveway, to my daughter, layan.

To… …….. All members of my family, my brothers and sisters, for love and appreciation

To all of helped me in completing this work to all of them I dedicate this modest work .

Ghadeer Yahya Mahmoud AL- Sarsour

Declaration

I hereby that this thesis submitted for the degree of Master of Science in physics is the result of my own research , except where otherwise acknowledged , and that this thesis (or any part of the same) has not been submitted for a higher degree to any other university or institution.

Signed:- …….

Ghadeer Yahya Mahmoud AL- Sarsour

Date:- 6 / 6 / 2015

E-mail : galsarsour@yahoo.com

Acknowledgement

Thank God Most Merciful the Graceful, who granted me the ability, and courage to accomplish this work.

I would like to express my profound gratitude to my research advisor, prof, Dr. Imad Al-Barghouthti for this guidance, patience and continuous support through all stages of this work. I would like also to extend my thanks to faculty and staff at the Physics department for their help and support during my graduate work. And special thanks for Mr Saed shahin and Mr Hamza Abudayyaeh for helping me in developing the computer program.

I would like also to extend my thanks to my husband for help and support during my graduate work

Special thanks and deep gratitude and appreciation go to my mother for her support and encouragement through the whole period of my study. last, but not least ,my heartfelt thanks go to my and family specially brothers and sisters ,for their lightened with love every step toward this work.

Abstract:

One of the most important solar-terrestrial interaction results is ion outflow at higher altitudes. The energization of ions, due to interaction with electromagnetic turbulence (i.e. wave-particle interaction), has an important influence on H^+ and O^+ ions outflows in the central polar cap and cusp regions. The effects of wave–particle interaction on H^+ and O^+ ions outflow in the central polar cap and cusp regions are investigated by using Monte Carlo method and Barghouthi model. The method includes the effects of wave-particle interaction, gravity, polarization electrostatic field, and divergence geomagnetic field within the simulation tube (1.7 - 14.9 R_E). The effect of altitude wave-particle interaction are taken into account by perturbing the ion's velocity with random increment($\Delta v_\perp$), such that $(\Delta v_\perp)^2 = 4D_\perp \Delta t$, where D⊥ is the diffusion coefficient and (Δt) is the time step.

In chapter three, we have used Nilsson et al (2013) diffusion coefficients, calculated from Cluster mission observations, to obtain the altitude behavior of O^+ and H^+ ions outflow, and in chapter four we have compared between these simulation results and simulation results obtained by using Barghouthi (1997) and Barghouthi et al. (1998) diffusion coefficients calculated from Dynamics Explorer spacecraft (DE-1).

It is very obvious that there is a big difference between both simulation results due to different diffusion coefficients; this difference is attributed to the altitude behavior of the diffusion coefficient and to the orbit of the spacecraft. We can say that the numerical values due to DE-1 satellite are much higher than the corresponding values due to Cluster spacecraft. These discrepancies are due to the orbit of the satellite and to different geophysical conditions.

Table of contents

List of figures

Title **page**

Title **page**

List of photos

Title page

LIST OF ABBREVIATIONS

- **WPI:** Wave-Particle Interaction**.**
- **Fig** : Figure.
- **MC :**Monte Carlo .
- **Eq :** Equation.
- **IMF:** Interplanetary Magnetic Field
- **N :**Nilsson
- **B :** Barghouthi
- **DE-1:**Dynamic Explorer 1 satellite`
- **Cpc** :central polar cap

Chapter one

General Introduction:

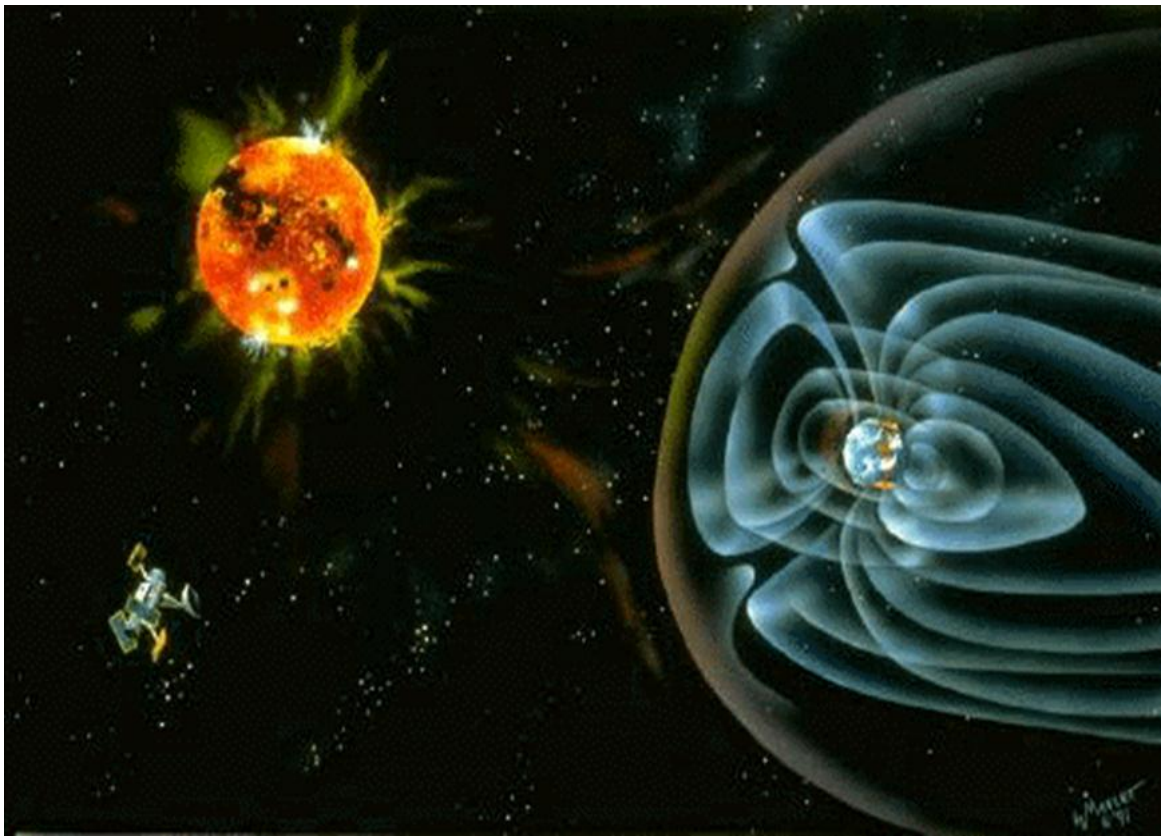

Photo (1.1): An artistic illustration of the Sun, the solar Wind and geomagnetic field.

Note that the scale of the image is far from being realistic Source: http://www.nasa.gov

(1-1) **Introduction:**

The Earth is one of the planets that have a strong magnetic field, to describe the shape of the earth magnetosphere; we must first discuss phenomena caused by the sun. the sun emits charged particles continuously from its extremely hot atmosphere. These charged particles are mostly electrons and protons, that are produced from the thermonuclear reactions inside the sun.

The energetic particles and the sun magnetic field that they pull into space are called the solar wind. The magnetosphere is the place of dynamic interaction between the solar wind and the earth plasma.

The Earth and its atmosphere are embedded in the magnetosphere, a region in space dominated by the geomagnetic field, shielding our planet as it deflects the energetic solar wind [Axford, 1968].

The high-latitude region, into which the open magnetic field lines of the lobes are mapped, is called the central polar cap, and the most recently opened field lines, are known as the cusps and night side.

The earth's magnetic field would resemble a simple magnetic dipole, except that the solar wind distorts its shape. much like a big bar magnetic field as illustrated below fig(1.1), the solar wind stretches the earth's magnetic field into a bullet shape, forming the large cavity known as the "magnetosphere." The magnetosphere is that region dominated by the magnetic field. Close to the earth's surface the approximates a dipole field, but further out the field becomes increasingly distorted.

(1.2)The structure of the magnetosphere:

The magnetosphere is the place of dynamic interaction between the solar wind and the earth plasma. Is blunt on the sunward side, extending out 10 to 12 R_E, earth radii (64,00Km), toward the sun. The magnetosphere also has a long tail on the anti-sunward 75,000 side, extending thousands of Earth radii (millions of Kilometers) in the direction away from the sun.

This portion of the magnetosphere is called the "magnetotail". Although much of the magnetosphere is nearly a perfect vacuum, its huge size allows energy in the solar wind to

drive electric currents and set plasma in motion within the magnetosphere and earth's upper atmosphere.(http://en.wikipedia.org/wiki/Magnetosphere)

(1-3) Structure of the Outer Magnetosphere:

Bow shock, since the solar wind is fully ionized plasma and carried with it a magnetic field, the Interplanetary Magnetic Field (IMF) it cannot cross into the earth's magnetic field, but it can distort it.

The bow shock is the shock front when the solar wind is suddenly slowed from supersonic to sonic speeds Plasma that has built up at the nose of the magnetopause. The bow shock marks the transition from undisturbed to turbulent solar wind flow.

The Bow shock is much like the aerodynamic shock wave that forms when a blunt object is placed in supersonic flow.

Magnetopause is the boundary between the confined planetary magnetic field and the solar wind plasma in the magnetosheath. The magnetopause is the surface at which the particle pressure of the advancing solar wind plasma is balanced by the earth's magnetic field pressure.

In other words, the magnetopause marks the boundary of separation between the IMF the earth's magnetic field .Solar wind plasma cannot easily cross the magnetopause. The location of the magnetopause changes as the speed of the solar wind changes (10_12) R_E down to(6_7 R_E).

The magnetosheath is the region of turbulent solar wind plasma located between the bow shock and the magnetopause. The plasma is compressed and heated at the nose of the Magnetopause but accelerates in the antisolar direction as it moves around the magnetosphere. The IMF in the magnetopsheth is also disturbed from its original orientation in the ambient solar wind.

The magnetotail is that region where the earth's magnetic field lines are drawn back in the antisolar direction by the motion of the solar plasma attempting to pass around the magnetopause. (http://en.wikipedia.org/wiki/Magnetosphere)

The solar plasma draws the tail backward for millions of Kilometer where it eventually becomes indistinguishable from the IMF. Beyond about 10 R_E the magnetic field lines of the earth's field are essentially parallel to those of the IMF.

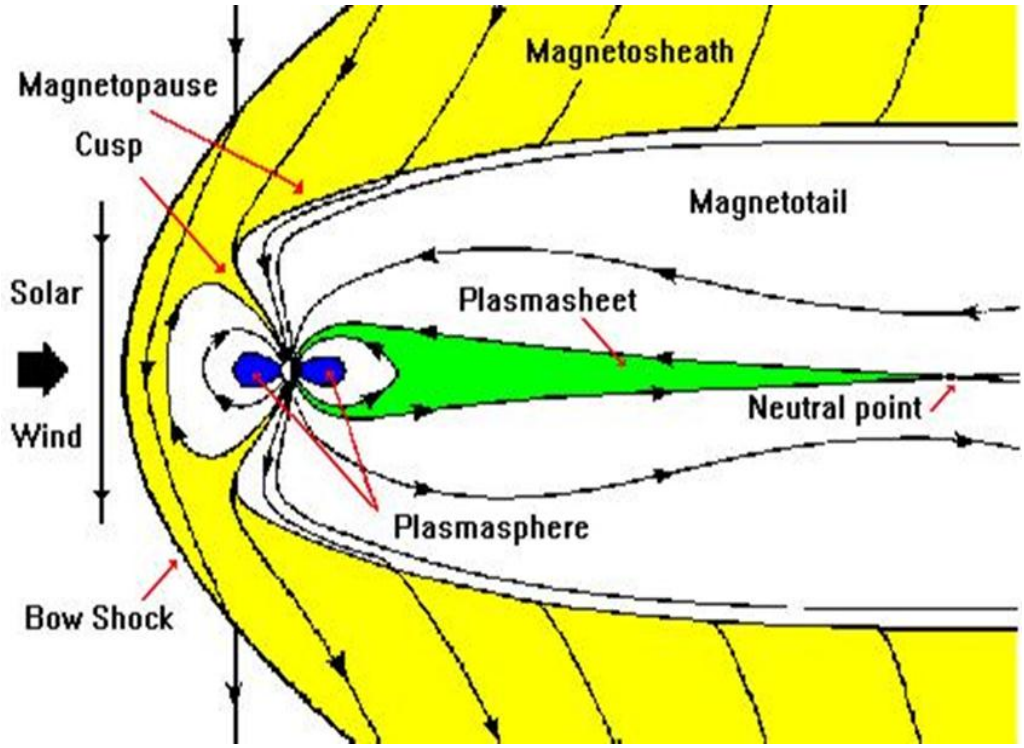

Figure (1.1) : Schematic illustration of the magnetospher including important parts and

Boundaries like bow shock, magnetosheath, magnetopause, the cusp, plasmasphere, magnetotail (Philips Astronomy Encyclopedia,2002).

The magnetopause separates the confined planetary magnetic field and magnetospheric plasma from the magnetized solar wind plasma in the magnetosheath. The location of the magnetopause is determined by balance between the solar wind hydrodynamic pressure and the magnetic pressure of the compressed planetary magnetic field and is generally characterized by a discontinuity in the tangential component of the magnetic field. The tail-like is seen in fig (1.1) allows the ions (thermal plasma) long to escape along these field lines in the tail, [Desseler and Michel,1966, Bauer,1966]. The outflow of plasma through regions of open magnetic field lines, resulting in a permanent escape of ions from the polar ionosphere is called polar wind, and the hydromagnetic model later proved that the out flow should be supersonic [Axford, 1968].

(1-4)Polar structures:

The polar cusps are two small regions where the earth's magnetic field is perpendicular to the magnetopause.One each exists above the magnetic poles of the earth. This geometry allows a trickle of charged solar wind protons and alpha particles to directly enter the magnetosphere**.**

The polar cap,the solar wind particles that enter the polar cusps are funneled along magnetic field lines straight to the earth's atmosphere where they ionize atoms and emit light.

The polar cap is one of the most tenuous regions within the magnetosphere. Its equator ward boundary, however, does not appear as a steep density decline because equally low densities can be detected in the auroral zone. In summer at low altitudes, the polar cap density is quite high in the central polar cap, that is, of the same order of magnitude as at lower latitude, while this is not observed in winter or at high altitudes.

The central polar cap is the area around the geomagnetic poise bounded by the aurora ovals, as shown in fig (1.2). Polar cap are high altitude region on both hemispheres with open magnetic field line connecting directly to the inter planetary magnetic field. In addition, polar caps from one of the ionospheric sources of magnetospheric plasma. This is due to the so-called polar wind, first suggested from theoretical arguments [Banks and Holzer,1968] [Axford,1986]. The defining classical polar wind characteristics are that it is cold, field-aligned (out of the ionosphere) ,and the velocity are inversely corrected with ion mass, favoring lighter ions (i.e. H and He), [Banks and Holzer,1969]. later observations have revealed some new features in the polar wind.

The cusp is the region where the solar wind plasma has direct access to the Earth's environment **[**Smith and Lockwood, 1996]. In the magnetosheath, the average solar wind density is (50_100) cm^{-3}, which is an order of magnitude higher than densities in the outer regions of the dayside magnetosphere. Thus, the density should be relatively high in the cusp.

The cusp properties, such as the electron density and the location, change significantly from orbit to orbit. A typical density is between 40 and 100 cm^{-3} in the high-altitude (4-8R_E)

cusp. Based on individual cusp crossing, we found several cases where the cusp can assume a new position, responding almost instantaneously to changes in the IMF orientation.

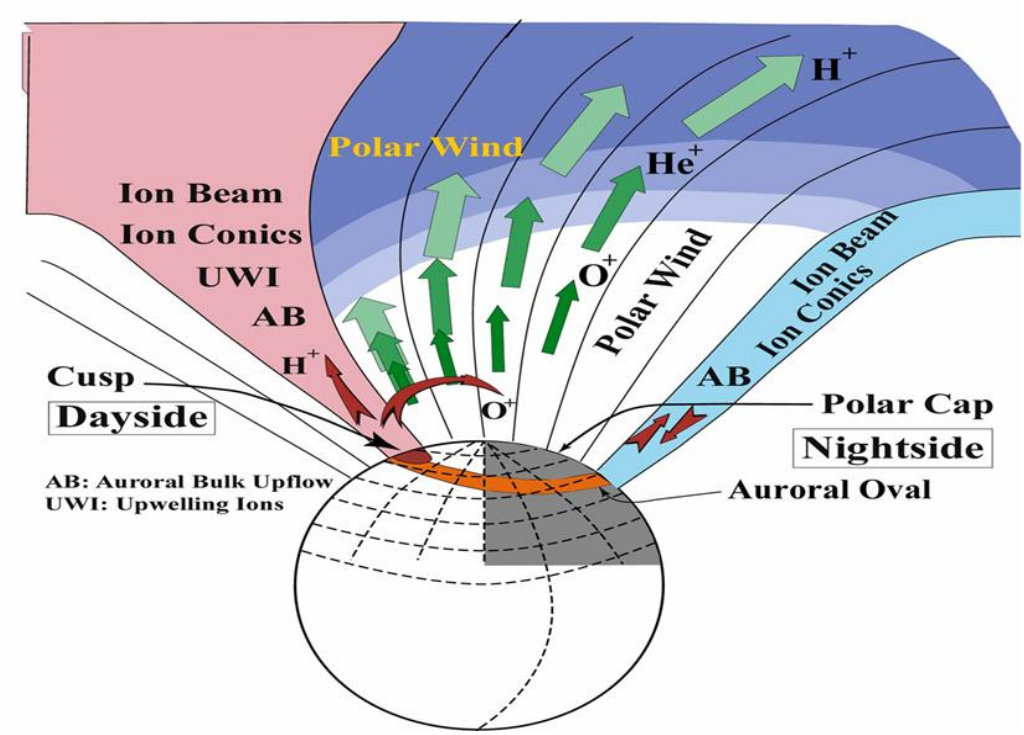

Figure (1.2): Schematic diagram of polar wind flow in the polar cap in the northern hemisphere and cusp, nightside regions.

http://ssdoo.gsfc.nasa.gove /education/lectures /fig12.gif

(1-5) Previous studies:

Several studies have been conducted of the effects that WPI have on ion outflow. The effect of WPI were first studied in the auroral region, because the observed levels of wave turbulence there are several orders of magnitude larger than those measured in the polar cap [Gurnett et al.,1984]. [Chang et al .,1986] and [Retterer et al .,1987] used a Monte Carlo simulation to study the perpendicular heating of O^+ due to a cyclotron resonance with broadband electromagnetic turbulence (i.e. wave particle interaction) . An imposed wave spectral density was used that was constant with altitude, and O+ conics were formed that had characteristics which were in agreement with the measurements.

Another series of studies [Bouhram et al., 2002, 2003a , 2003b , 2004] investigated the transverse heating and out flow of ions in the cusp cleft region.

[Bouhram et al., 2002] studied the spatial properties of ions sphere ion outflows associated with perpendicular heating processes in the cusp using a conjunction study from two perpendicular heating processes in the cusp using a conjunction study from two satellites and ground radar system, they presented an event of low energy outflowing H^+& O^+ populations observed by the Hyperboloid experiment aboard Inter ball Auroral Probe from 13.000 to 19.000 km altitude, and these populations are observed by the day side morning polar cap.

[Bouhram et al., 2003a] developed a two dimensional Monte Carlo trajectory based code for ion outflow from the day side cups cleft, which is associated with transverse ion heating, and they modeled the altitude dependence of ion cyclotron resonance heating from 1000 km to 3 R_E by a power law spectrum with an index α and a parameter that is proportional to the spectral density at a low frequency.

[Bouhram et al., 2003b] use high - altitude (1.5-3 R_E) ion observation as constraints and the results of [Bouhram et al, .2003a] are used to determine the altitude depended of transverse ion heating during a significant number of the Interball-z satellites.

[Barqhonthi, 1997] obtained an altitude dependent diffusion coefficients and [Bouhram et al., 2004] derived velocity dependent diffusion coefficient you do it use a combined (altitude part from [Barghouthi, 1997] and the velocity part from [Bouhram et al., 2004]) from for the diffusion coefficient to investigate the H^+ and O^+ ions outflow in the

equatorward of the cusp. And also, are you going to do it develop a model for the velocity diffusion coefficient $D_{\perp}$ to be velocity dependent (based on the work of [Crew and Chang,1985][Change ,1993,and Retterer et al .,1994])and altitude dependent (based on the work of [Barghouthi , 1997 and Barghouthi et al., 1998]) you do it use developed model of the diffusion coefficient to study the effect of velocity and altitude dependent ware particle interaction on O^+ and H^+ ions out flows in the Auroral region .[Barghouthi et al.,2011] study the H^+ out flow in the polar wind.

And also , in this work , we will the $O^+$and H^+ ions outflow in the central polar cap and cusp regions by using [Nilsson et al,2013] diffusion coefficients, also we are going to compare between the Simulation results obtained by using [Nilsson et al,2013]coefficients with the corresponding results obtained by [Barghouthi (1997)] and [Barghouthi et al., (1998)].

(1-6) Statement of the problem:

We are going to investigate the $O^+$and H^+ ions outflow in the central polar cap and cusp regions by using [Nilsson et al,2013] diffusion coefficients, also we are going to compare between the Simulation results Obtained by using [Nilsson et al,2013] coefficients with the corresponding results obtained by [Barghouthi (1997)] and [Barghouthi et al (1998)].

As a result of this comparison, we are interested to provide the space physics community with appropriate diffusion coefficient in each region and for each ion.

Chapter two

Theoretical Formulation

Chapter two

Modeling O^+ and H^+ ion outflows: Ionospher –magnetosphere coupling

(2.a) Introduction:

From ionosphere (the ionized upper part of the atmosphere) ion outflows occur at high latitudes above the geomagnetic north and south poles. The ions (mainly O^+ and H^+) escape along semi-open geomagnetic field lines extending anti-sunward to large distances from the core of the Earth. In other words, the ions escape out from ionosphere into the magnetosphere. In other words, the Earth's atmosphere constantly loses matter to the surrounding space through different outflow processes. Many theoretical studies have been devoted to investigate the H^+ and O^+ ions outflows at high-altitudes and high-latitudes regions, in particular they were interested in explaining the ions acceleration in polar wind and auroral regions. These studies were motivated by the existence of energetic O^+ ions at high altitudes that have been confirmed by Gurgiolo and Burch [1985], the observations of the Suprathermal Mass spectrometer (SMS) aboard the Akebone satellite [Abe et al., 1993] which showed a significant mean outflow velocity for O^+ ions at low altitudes (5000 km) and a monotonically increasing altitude profile for O^+ ions above 5000 km. Also, the observations of non-Maxwellian ion velocity distributions such as elevated conics and toroids that have been observed by Winningham and Burch [1984], and Huddleston et al. [2000].

Several studies explained these observations in terms of the classical polar wind theory, however many other studies explained it in terms of the non-classical mechanisms (e.g. wave-particle interactions, parallel potential drops, centrifugal accelerations, etc…) in the polar wind theory [Tam et al., 2007]. In this study, we are interested in the mechanism of wave-particle interactions (WPI) and its significant role in heating the ions in the direction that is perpendicular to the geomagnetic field and consequently, part of this gained energy is converted into the parallel direction due to the mirror force. This process produces O^+ and H^+ acceleration in the polar wind region and auroral region.

We have previously carried out Monte Carlo simulations of the ions outflows that considered the effect of WPI, in addition to the effects of gravity, polarization electric field, and diverging geomagnetic field, and compared these with the corresponding observations

in both regions [Nilsson et al., 2012. 2013, Barghouthi et al., 2011, 2014, and Barghouthi, 2008].

(2.b) Survey of the field:

In a series of simulation studies, [Barakat and Barghouthi, 1994a, b; Barghouthi and Barakat, 1995; Barghouthi, (1997); Barghouthi et al., (1998); Barghouthi and Atout, (2006); Barghouthi et al., 2007; Barghouthi et al., 2008; and Barghouthi, 2008] used Monte Carlo approach in which the effects of gravity, polarization electric field, and geomagnetic field were included, to investigate the effect of wave particle interactions on the H^+ and O^+ ions outflow in the polar wind region. They conclude that the effect of finite gyroradius is the reason for produce of the H^+ and O^+ ions toroids at high altitudes above the polar cap, that are observed by TIDE and TIMAS ion instruments on board the polar spacecraft. In addition they found that, the O^+ ions are preferentially heated because of higher mass and owing to the pressure cooker effect, furthermore, they conclude that the effect of the body forces is more important in the polar wind region than their effect in the auroral region on ions, and also, the effect of the body forces on O^+ ions is more important than that on H^+ ions. Furthermore, they found that the ions are more energetic in the auroral region than in the polar wind region. In addition, they modify the formula for diffusion coefficient ($D\perp$) to take into account the effect of finite Larmor radius and used it to study the H^+ and O^+ ions outflow in the polar wind. [Yau et al., 2007] review the history of development of polar wind models and theories and they offer statistical studies or surveys of polar wind ions observations using data from ten or more satellite orbit passes, these observations were made from the ISIS-2, DE-1, Akebono, and POLAR satellites over the altitude range of 1,000 to 50,500 km, and spanned different phases of solar cycle, and they form a composite picture of the polar wind. More recently, [Nilsson et al., (2004, 2006, 2008a,b)] and [Arvelius et al., 2005] have been able to show the importance of the cusp origin ion outflow for the total ion outflow. The measurements were made at high altitude, about 10 earth radii, with the European Space Agency's Cluster spacecraft. The ion data combined with electric field data shows that heating must be much more effective at such high altitude as compared to magnetospheric mid-altitude (5 Earth radii), and even more so compared to low altitude (a few 100 km as for Freja and FAST spacecraft). The role of the initial ionospheric up flow for the total ion outflow has been assessed quantitatively [Nilsson et al., 2008b], as well as the role of centrifugal acceleration [Nilsson et al. 2008a]. The next

step in explaining the statistical results reported in [Nilsson et al., 2006] is to assess the perpendicular ion heating. This is where the Barghouthi model would be a perfectly matched tool to further improve our understanding.

(2.c) Barghouthi model

Barghouthi model has been described and developed in a series of paper [Barghouthi and Barakat, 1995; Barakat and Barghouthi, 1994 a, b; Barghouthi, 1997;Barghouthi et al., 1998, 2007, 2008; Barghouthi and Atout, 2006]. To be specific, the effect of wave-particle interactions on the polar wind plasma [Barghouthi et al., 1998] and as a result of perpendicular heating, are as follows; the temperature anisotropy $(T_{\perp} / T_{\parallel})$ was reduced and even reversed at high altitudes; the escape flux of O^+ ions could be enhanced by more than an order of magnitudes while the H^+ flux remains constant. The O^+ ions were heated more efficiently than H^+ ions, ion velocity distributions displayed conic behavior at low altitudes and because of finite gyroradius effect, the ion velocity distribution moved from conic to toroid at high altitudes.

In the auroral region, Barghouthi and Atout [2006], and [Barghouthi et al. 2007, 2008] investigated the effect of wave-particle interaction on H^+ and O^+ ions outflows at high altitudes related to the cusp by using the Monte Carlo method. They discussed the ion outflow by taking into consideration the effect of the finite gyroradius; they found that the behavior of ion outflow is completely different below and above the saturation point, (i.e. when the ion gyroradius becomes comparable to the wavelength of the electromagnetic turbulence). Below the saturation point, the ion velocity distribution displayed conic features, while above the saturation points it displayed toroidal features because of self-limiting heating process, in which the ions tend to move out of the heating zone in the velocity space. The presence of toroids is therefore a good signature that wavelength-limiting effects are important. This would allow for an experimental survey of upper bounds of the wavelength of electromagnetic turbulence.

Barghouthi [2008] compared between the simulation results for H^+ and O^+ ions outflows in the auroral region obtained by using three different forms for the velocity diffusion rate perpendicular to the geomagnetic field lines [Barghouthi and Atout, 2006; Barghouthi et al.,2007, 2008] with the corresponding observations and found that, the velocity diffusion rate perpendicular to the geomagnetic field lines obtained by Barghouthi and consequently,

Barghouthi model was appropriate for modeling ion outflow along auroral field lines. In specific, the simulation results obtained by using Barghouthi model, i.e. ion velocity distributions, temperatures, velocities, total energies, etc. were in excellent agreement when compared with a number of corresponding observations. Recently, as shown in figures (2.1), figure (2.2) Barghouthi et al. (2011) and Nilsson et al. (2013) used the Barghouthi model with the boundary conditions of the polar wind and auroral regions and obtained simulation results for H^+ and O^+ ions outflows in both regions and compared between simulation results and many different observations obtained from various satellites at different altitudes. These comparisons and similar ones enhance our understanding of the planet Earth's space.

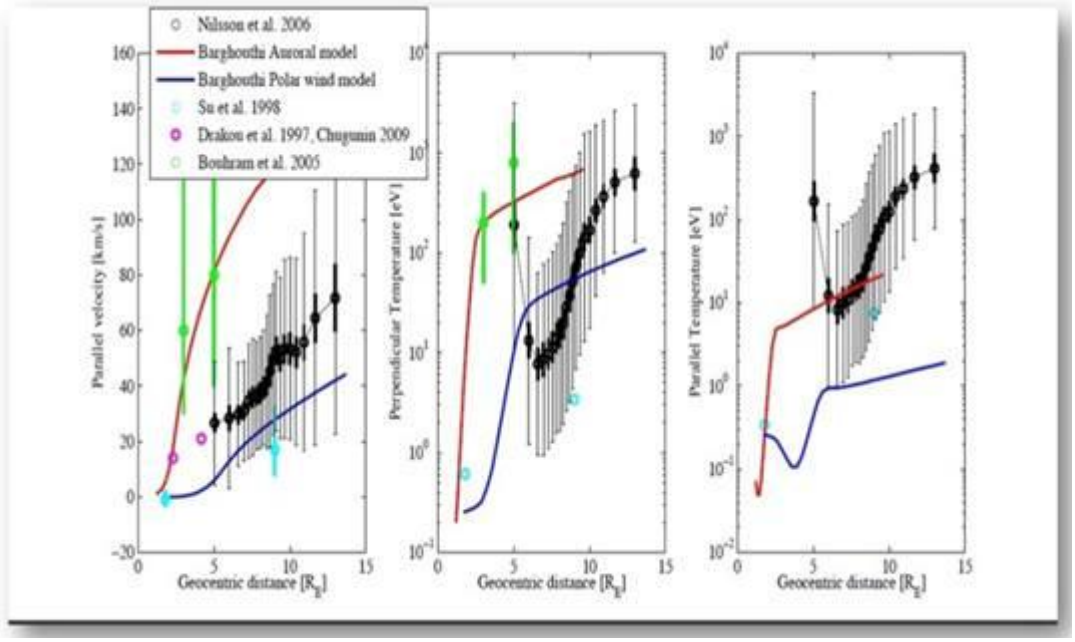

Figures (2.1): Altitude profiles for O^+ ions moments obtained from Barghouthi model are compared to Cluster observations and other studies. Cluster observations (black circles with error bars) compared with model results from Barghouthi auroral model (red curve) and polar cap model (blue curve). Thick black error bars indicate a 95% confidence interval for the mean, whereas thin black lines indicate the standard deviation. Results from other studies are indicated with colored symbols. (Nilson et al .,2013)

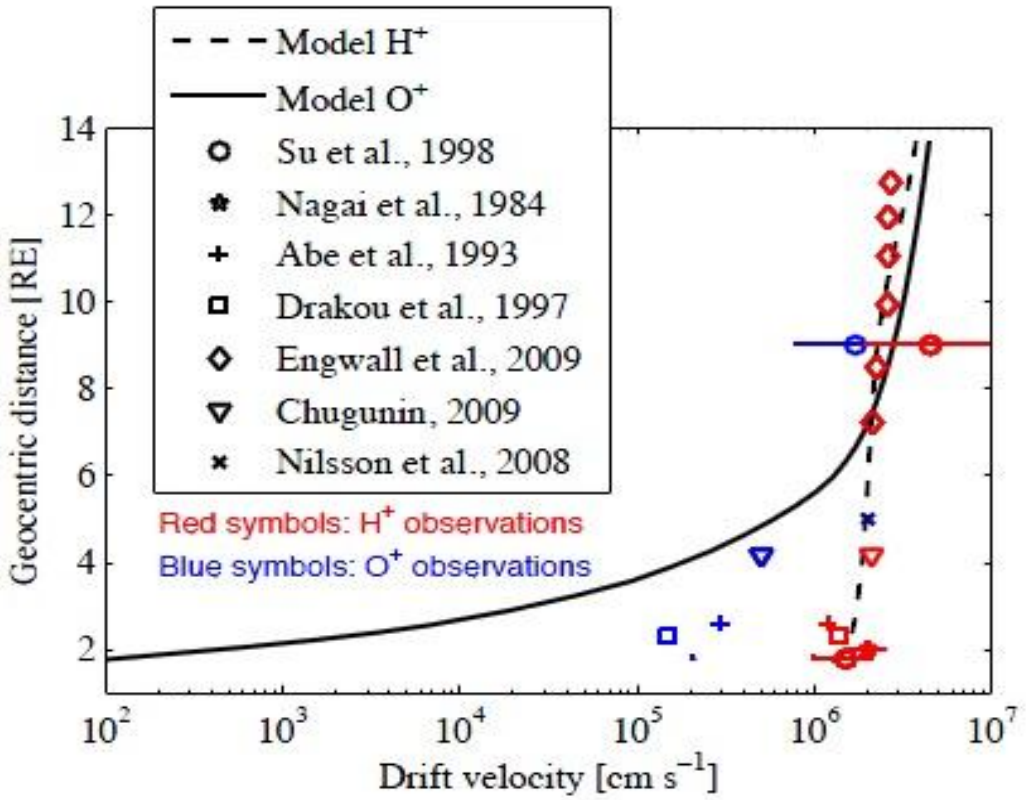

Figure (2.2): Altitude profiles of the drift velocity moments for O^+ ions (solid line)and H^+ ions (dashed line) when electromagnetic wavelength equals to 8 km. Different corresponding observations are marked on the profile. (Barghouthi et al .,2011)

(2.1) Boltzmann equation:

The Boltzmann equation is rate of change of the distribution function under many external forces and collisions, which describes each species in separate distribution function [Bellan et al., 2004]

Plasma is the fourth state of matter in addition to gas liquid, and solid. Which consist of free charge (i.e . ions, electrons and neutral atoms). The motion of these species under the effect of the influence of external force (gravitational, electric, polarization and magnetic] and the net collision of species in plasma we can deal with a separate velocity distribution function f_s (v_s, r_s , t) which defined such that f_s (v_s, r_s , t) dv_s dr_s represent the number of particles of species at time t which have velocity between v_s and v_s+ dv_s, and position r_s and r_s+ dr_s .

The evolution in time change the distribution function (i.e.change of v_s, r_s) because of the net effect of many external force and the net collision of species, which can be described by Boltzmann equation [Schunk, 1977]

$$\frac{\partial f_s}{\partial t} + \mathbf{v}_s . \nabla f_s + [\mathbf{g} + \frac{e_s}{m_s}(\mathbf{E} + \frac{1}{c}\mathbf{v}_s \times \mathbf{B})] . \nabla_{vs} f_s = \frac{\delta f_s}{\delta t} \qquad \text{.....(2.1)}$$

Where g is the acceleration of gravity, (E) is the electric field (B) is the magnetic field (e_s , m_s) are the charge and the mass of the species s respectively$\frac{\delta}{\delta t}$ is the time derivaties, c is the speed of light (∇) is coordinate space gradient, (∇vs) is the velocity space gradient.

The right hand side of Boltzmann equation
($\frac{\delta fs}{\delta t}$) represents the rate of change of f_s (v_s, r_s ,t) in a given region of phase space (v_s, r_s) as a result of collision .

As far as the collision and the inverse power potentials, is given by Boltzmann collision integral [Schunk , 1977]

$$\frac{\delta df_s}{\delta d_t} = \sum_t \int d^3 v_t d\Omega g_{st}\, \sigma_{st}\, (g_{st}, \theta)[f_s^1\, f_t^1 - f_s f_t] \qquad \text{.....(2.2)}$$

Where dΩ is the element of solid angle in the s particle reference frame. θ is the scattering angle, g_{st} is the relative velocity of the colliding particles s and t , d^3v_t is the volume

element in the velocity space, σ_{st} (g_{st} ,θ) is differential scattering cross section, and the prime denote quantities evaluated after collision.

(2.1.1) The gravitational force:-

Newton's law of gravity states that every particle in the universe attracts every other particle with a force that is directly proportional to the product of their means and inversely product proportional to the square of the distance between them, regardless of the medium that separates them .If an ion have mass (m) separated by a distance (r)from the Earth whose massμ_e the gravitational force is.

$$f(r) = -\frac{G\,\mu_e m}{r^2}\ \hat{r} \quad \ldots\ldots\ldots\ldots\ldots\ldots (2.3)$$

Where G is a universal constant called the universal gravitational constant, $\hat{r}$ is aunite Vector directed from the center of the Earth to the ion, μ_e is the Earth mass, and the negative sign indicates that the gravitational force is attractive, Therefore, the ion is attracted to the Earth.

The acceleration of gravity commonly is denoted by (g), which is produced by gravitational force from the Earth on the ion

g is given by :-

$$g = \frac{F}{m} = -\frac{GMe}{r^2}\,\hat{r} \quad \ldots\ldots\ldots\ldots\ldots\ldots (2.4)$$

The gravitational potential energy Φ_g (r) can be found from the definition of work done by the force:-

$$w = -\left(\Phi_g - \Phi_{g_o}\right) = -\Delta\emptyset(r) = -\int_{r_0}^{r} F(r).\,dr \quad \ldots\ldots\ldots (2.5)$$

Where r_o and r are the geocentric distance to the location of the ion ,Φ_g and Φ_{g_o}represents the gravitational potential energy at altitudes r_o and r , but from the above we can found the formula of gravitational potential energy as a function of v by substitute F(r) from equation

(2.3) into the equation to get :-

$$\Delta\emptyset g(r) = -G\ \mu_e\ m \int_{r_0}^{1} \frac{dr}{dr^3} = G\mu_e m\ (\frac{1}{r_0} - \frac{1}{r}) \quad \ldots\ldots\ldots\ldots (2.6)$$

Where r is the distance separated the Earth _ion system and provided that $r > r_o > R_E$

(2.1.2) Polarized Electrostatic Field:-

By the geomagnetic field the charged particles,i.e. electrons and ions will move along the field lines, there is a clear difference of mass between them so the gravity leave electrons arise more than the heavy ions, that make a slight charge separation forming polarized electrostatic field, electrons then moving due to temperature and density gradient and gravity. To describe the plasma outflow after many approximation like diffusion approximation were done to reach the momentum equation for electrons [Schunk and Naqy , 2000]]

$$\Delta_{\|} P_e\ + (\Delta . t_e) + n_e\ eE_{\|} - n_e m_e g_{\|}$$

$$= \ n_e m_e v_{ei}(u_i - u_e) + n_e m_e v_{en}(u_n - u_e)_{\|} \ldots\ldots\ldots\ldots (2.7)$$

Where p_e is electrons partial pressure, E‖ the polarization electrostatic field that develops due to the very slight charge separation, n_e is electron density, $m_e$is the mass of electons, $g_{\|}$ is the component of a cceleration due to gravity along the geomagnetic field line.$v_{ei}$is the collision frequency, and u_i is the dift velocity of ions and u_e is the dift velocity of electrons, $v_{en}$is the electrons and neutral atoms collision frequency at the moment of collision .

However in many applications it is needed to get the electrostatics potential (V_E) can be obtained from an explicit expression. For the electric field created owing to the movements of electrons.

Can be obtained from equation (2.7) under some conditions, which are the terms containing m_e is neglected since the mass of electron is small.

In addition, the electron ion collision term is dropped, Therefore equation (2.7) can be written as:-

$$eE_{\|} = \frac{1}{n_e}\nabla p_e \quad \ldots\ldots\ldots\ldots\ldots\ldots (2.8)$$

The expression is valid regardless of the number of ion species in the plasma.

It is valid to write $E_{\|} = -\Delta_{\|} V_E(r)$, due to alternate form of isothermal electron gas and letting $E_{\|} = -\Delta_{\|}\emptyset$ and $p_e = n_e kT_e$, is the potential energy to the polarization electric field and assuming that T_e is constant so we can write equation (2.8) as :-

$$\frac{e}{kT_e}\frac{\delta V_E}{\delta r}(r) = \frac{1}{n_e}\frac{\delta n_e}{\delta r} \quad \ldots\ldots\ldots\ldots\ldots\ldots (2.9)$$

Where r is the spatial coordinate either along or perpendicular to geomagnetic field (B).

However to find the electrostatic potential (V_E), we treat equation (2.9) by integrating it and the result is called Boltzmann relation :-

$$n_e = (n_e)_o e^{\frac{eV_E}{kT}} \quad \ldots\ldots\ldots\ldots\ldots\ldots (2.10)$$

Where$(n_e)_o$ is the equilibrium electron density that prevails when V_E=0 but now we can write. The electrostatic potential (V_E) as

$$V_E(r) = \frac{KT_e}{e}\ In[\frac{n_e}{(n_e)_o}] \quad \ldots\ldots\ldots\ldots\ldots\ldots (2.11)$$

Due to this the polarization electrostatic potential energy $\Phi_E(r)$ is given by [Barghouthi2008]

$$\Phi_E(r) = kT_e\ In\ [\frac{n_e}{(n_e)_o}] \quad \ldots\ldots\ldots\ldots\ldots\ldots (2.12)$$

To summarize the final potential energy profile $\Phi_E(r)$ due to gravity and polarization electric field , we return to the above two sections , the potential energy causing body force (i. e .gravitational and polarization electrostatic) which is given by [Barakat and Schunk, 1982]

$$\Phi_E(r) = kT_e\ In\ [\frac{n_e}{(n_e)_o}] + G\mu_e m\ (\frac{1}{r_o} - \frac{1}{r}) \quad \ldots\ldots\ldots\ldots (2.13)$$

Where k is Boltzmann's constant, Te is electron temperature n_e and (n_{eo}) are the electron densities at r and (V) respectively G is universal gravitational constant, $\mu_e$is the mass of the earth and m is the ion mass.

(2.1.3) Charged particles in a magnetic Field:-

The known that when in ion with charge (q)moves with velocity v in a uniform magnetic field will be acted on by a famous force called Lorentz force , which is represented in Gaussian system of units as:

$$\boldsymbol{F} = \frac{q}{c}\,\boldsymbol{v} \times \boldsymbol{B} \ldots\ldots\ldots\ldots\ldots\ldots (2.14)$$

Where c is the speed of light. when appositive ion moves perpendicularly to a uniform magnetic field $\mathbf{B_o}$ the magnetic force (Lorentz force) can change only the direction of ion's velocity, with the same speed, so we will note the uniform magnetic field, The radius of the circular path is called Larmor radius (gyroradius), and it can be computed by equating between Lorentz force and centrifugal force to give :

$$a_L = \frac{mc}{q}\frac{v_\perp}{B} \ldots\ldots\ldots\ldots\ldots\ldots\ldots\ldots\ldots\ldots (2.15)$$

The quantity ($q\frac{B_o}{mc}$) is called the Larmor frequency, is known as:-

$$\Omega_c = q\frac{B_o}{mc} \ldots\ldots\ldots\ldots\ldots\ldots\ldots\ldots\ldots\ldots\ldots\ldots (2.16)$$

However, the path of positive ion in a uniform magnetic field is shown in Figure (2.1)

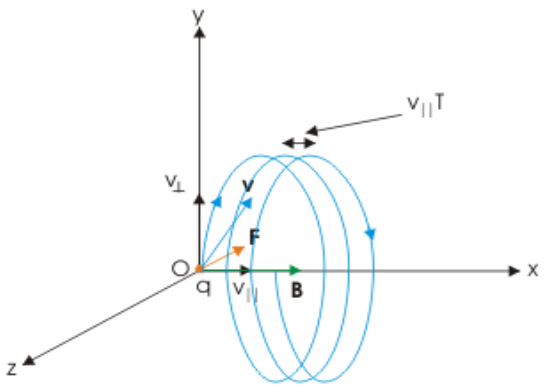

Fig (2.3): Helical path motion of a charged Particle in a uniform magnetic field

http://www.miniphysics.com/

The ion velocity vector can be analyzed into two orthogonal components, one paralled to B_o which represented by $v_{\|}$ and the other perpendicular to B_o which represented by $v_{\perp}$ so we can write it such that:-

$v = v_{\|} + v_{\perp}$……..(2.17)

Assume there is no force exerted on the ion in the parallel direction the uniform magnetic field ($B_{o)}$ this implies that the ion waves unimpeded with a constant $v_{\|}$ along the uniform magnetic field**.**

There is cyclotron motion was shown in fig (2.1) which is associated with the $v_{\perp}$ velocity component and with Larmor radius depends on the perpendicular velocity component.

In the cyclotron motion the magnitude of $v_{\perp}$ remains constant (uncharged) but the direction of the perpendicular velocity $v_{\perp}$ change continously in auniform magnetic field as shown in fig (2.1).

According to Lorentz force the Positive ions (i.e. O^+ , H^+) gyrate in an opposite direction of gyration for negative ions (i.e. electron) because the positive ions gyrate in left- hand sense relative to the uniform magnetic field B_0.To guiding center is central field line about which the ions gyrate.

When there is a strong magnetic field gradient in certain region the ion mirrored by Lorentz force at the moment in time when the ions is being mirrored, then a $v_{\perp} = v$ and $v_{\|} = 0$,which means all of its velocity is in the perpendicular to the magnetic field , The lorentz force has a component toward the left , which leads the ion to accelerate in adirection antiparallel to the magnetic field . But the lorentz force effects in a direction perpendicular to velocity vector, also there is no work done on the ion and the total energy of the ion remains constant as shown in the following equation:

$$E_T = \frac{1}{2}mv^2 = \frac{1}{2}mv_{\|}^2 + \frac{1}{2}mv_{\perp}^2 = E_{\|} + E_{\perp} \ldots\ldots\ldots\ldots\ldots (2.18)$$

Where E_T ,$E_{\|}$ and $E_{\perp}$ are the total. Parallel and perpendicular kinetic energy of the ion respectively.

However, for ion moves from left to right in a constant magnetic field , the gradient as shown in figure (2.4). When $E_{\perp}$ decreases, $E_{\|}$ increases, due to $E_{\perp}$is keeping constant. The

mirror point is reached, at $E_{\perp} = E_T$ and $E_{\parallel} = 0$, then the ion starts to be mirrored and so with $E_{\perp}$ decreasing and $E_{\parallel}$ increasing. by the mirror force The ion will be trapped due to a magnetic field lines and will bounce back and forth between mirror points.[Tsurntani and Lakhina, 1997]

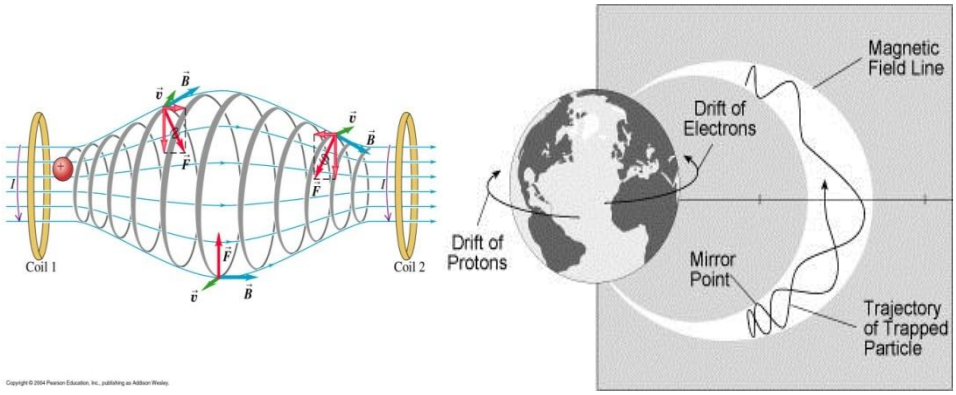

Figure (2.4) :magnetic bottles for plasma particles.

https://www.google.ps/search

(2.2) Wave-particle Interaction: (WPI)

The stability of plasma that is found in the Aurroral region and polar cap was the subject of many theoretical investigations; the result found that plasma is unstable with found respect to the variety of wave [Barakat and Schunk, 1989].

In the Auroral region the observed level of the electromagnetic turbulence occurred over the polar cap [Gurnett and Inan,1988]

The effect of (WPI) on ion out flows in the polar wind and aurora region is very important to investigate becomes the escape of the ionospheric ions to the magnetosphere is an important ionosphere magnetosphere coupling mechanism.

The effects of (WPI) are represented by particle diffusion in the velocity space is [Retterer et al.,1987 a]

$$[\frac{\partial f}{\partial t}]_{WpI} = \left(\frac{1}{v_{\perp}}\right)\frac{\partial}{\partial v_{\perp}}\left[D_{\perp}v_{\perp}\frac{\partial f}{\partial v_{\perp}}\right] \dots\dots\dots\dots\dots (2.19)$$

Where ($D_{\perp}$) is the quasi _linear velocity diffusion rate perpendicular to geomagnetic field lines. The given by the following expression [Retterer et al.,1987b]

$$D_{\perp} = \frac{q^2}{m^2} \sum_{n=-\infty}^{\infty} \int \frac{d\omega}{2\pi.} \int \frac{d^3K}{(2\pi)^3} \left[\frac{n\Omega}{\omega}\right]^2 A_n \, \pi \, \delta \, (\, \omega - n \, \Omega - k_{\parallel} v_{\parallel} \, \ldots \ldots \ldots (2.19)$$

$$A_n = \frac{1}{2} J_{n-1}^2 \left| E_L \right|^2 (k, \omega) + \left[\frac{v_{\parallel} J_n^2}{v_{\perp}}\right]^2 \left| E_{\parallel} \right|^2 (k, \omega)$$

$$+ \frac{1}{2} J_{n+1}^2 \left| E_R \right|^2 (k, \omega) \ldots \ldots \ldots \ldots \ldots \ldots \ldots \ldots (2.20)$$

In this Equation, q is ions charge, m is the ions mass, Ω is the gyrofrequnency, ω is the angular frequency of the electromagnetic turbulence, k is the wave vector.

$$j_n = j_n \left(\frac{K_{\parallel} V_{\parallel}}{\Omega}\right) \ldots \ldots \ldots \ldots \ldots \ldots \ldots \ldots (2.21)$$

Is the standard Bessel function and $\left| E_L \right|^2$and $\left| E_R \right|^2$are the spectral densities of the electric field in the two perpendicular polarization [Retterer et al.,1987b] assumed ($K_{\parallel} V_{\parallel}$<< Ω)

$$D_{\perp} = \frac{nq^2}{4m^2} [E_x(w = \Omega)]^2 \ldots \ldots \ldots \ldots (2.20)$$

Where $\left| E_L \right|^2 = \eta \left| E_x \right|^2 (w)$, $\left| E_x \right|^2$ is the spectral density of the wave, and η is the proportion of this density that correspond to left- hand polarized wave

The velocity diffusion rate ($D_{\perp}$) given in eq (2.22) is independent of velocity and its altitude dependence depend on the variation of ion gyrofreguency Ω.

(2.3)The Boundary conditions:-

We study the steady state flow of an ionized (H^+, O^+) along the geomagnetic field lines in the high altitude top side ionosphere (cusp, central polar cap and regions),the ions move under the effect of body force (i.e. gravitational and polarization ,electrostatic fields) and mirror force due to the divergence of the geomagnetic field hence, the simulation region is a geomagnetic tube extending from r= $1.7R_E$ to r=14.7 R_E as showing fig (2.3)

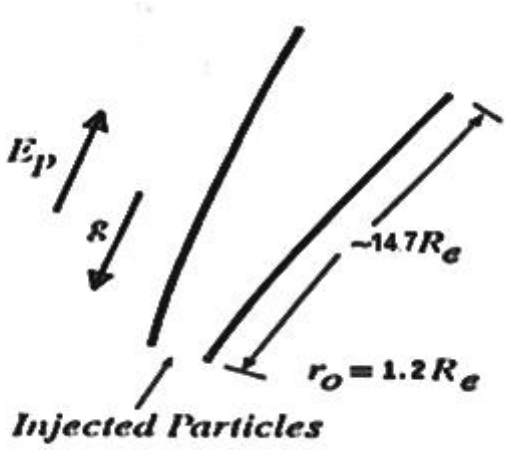

Fig(2.5):A schematic representation of the model considered by the Monte Carlo method **[** Barakat and Barghouthi , 1994 a, b]

The boundary conditions selected for O^+ ions at the lower altitude boundary were assumed to have a density and drift velocity of 10 cm^{-3} and 2 km/s respectively for the central polar cap and 10000 cm^{-3} and 0.5 km/s respectively for the cusp as suggested by (Nilsson 2013). H^+ ions at the lower altitude boundary were assumed to have a density and drift velocity of 34 cm^{-3} and 18 km/s respectively for the Central polar cap as suggested by (Nilsson 2013) and 200 cm^{-3} and 16 km/s respectively for the cusp as in Barghouthi(1997) Finally the simulation tube was extended to a large range of altitudes, namely from 1.7 R_E to 14.7 R_E in the central polar cap, and from 1.2 R_E to 15.2 R_E in the cusp. The temperature at the exobase was assumed to be 3000 K for both ions and electrons in all regions.

(2.4) Monte Carlo simulation:

Computer simulation is an essential tool in studying the space plasma physics. Simulation allows us to develop and test models, to evaluate approximate theories of space plasma, and to obtain detailed information about the ion velocity distribution function and its moments (i.e. density, drift velocity, temperature, heat flux ...) at different altitudes [Barghouthi et al 2003]. The plasma medium, such as the polar wind, ionosphere, magnetosphere, and plasmasphere, consists of ions, electrons and neutral atoms. The motion of these species under the effect of geomagnetic field, gravitational field, polarization electric field and the interactions between them is very difficult to understand. However, Monte Carlo simulation can offer detailed information describing the motion of the plasma constituents and some of the interactions between plasma species [Winkler et al., 1992]. In dealing with plasma it is convenient to describe each species in the plasma by a separate velocity distribution function. The evolution in time of the species velocity distribution function is determined by the net effect of collisions and the flow in phase space of species under the effect of external forces. The mathematical description of this evolution is given by the well-known Boltzmann equation [Schunk 1977].

The Monte Carlo method was shown to be a very powerful technique in solving the Boltzmann equation by particle simulation. It's simple concept, straightforward algorithm, and its adaptability to include new features (such as, gravity, electric field, geomagnetic field, and different collision models) make it useful tool in space plasma physics, and a powerful test of results obtained with other mathematical methods [Barakat and Lemaire, 1990]. Monte Carlo method has the advantage that one follows the motion of the individual particles and, hence, a lot of the important physics can be included self-consistently [Takisuka and Abe, 1977]. The standard procedure of the Monte Carlo simulation is to follow the motion of one ion under the effect of external forces and for a large number of collisions, and to continually monitor its velocity. Then, various kinds of time averages for the ion are computed, which can be equal to the corresponding ensemble averages of the system [Barakat et al., 1983]. In practice, the ion motion is simulated as follows. An ion is injected in to the simulation region with an initial velocity that is randomly generated such that it is consistent with the ion velocity distribution function immediately below the simulation region. The time interval between every two successive collisions is found via a proper random number generator. The ion trajectories during these intervals are determined

by the classical laws of motion of a charged particle under the influence of gravitational, electric, and geomagnetic fields. Changes of ion's velocity due to collisions are determined using another set of random numbers having the statistical properties determined according to the chosen collision model [Hubert and Barakat 1990]. Then a suitable grid in velocity space at different altitudes in the simulation region is used to register the ion's behavior. The time that an ion spends in each bin, divided by the bin's volume, is taken to be proportional to the ion's velocity distribution function at its center. Moreover, the individual segments of the trajectory can be directly used to find different velocity moments (i.e. density, drift velocity, temperature, heat flux...).

We have used Monte Carlo method to solve Boltzmann equation in ionosphere, magnetosphere, polar wind and auroral regions [Gaimard et al 1998, Barghouthi, 2005, Barghouthi, 2008, Barghouthi et al 2011, and 2013].

Chapter Three

The results

Chapter three

The results

(3.1) Introduction:

The effects of gravitational field, polarization electrostatic field, geomagnetic field, and altitude dependent and wave-particle interaction on H^+ and O^+ ions outflow in the two regions, central polar cap and cusp. have been investigated by using Monte Carlo simulation .

(3.2) The results in central polar cap region:

(3.2.a) O^+ ion:

To study the effect of wave particles interaction on the O^+ ion in the central polar cap, we computed the distribution function $f(O^+)$ at several altitudes extended from 1.7 to 14.7R_E

Fig (3.1) presents contour plots for O^+ velocity distribution at different altitude dependent and WPI in the central polar cap region.

At the injection point 1.7R_E and 1.8 R_E is half –non drifting Maxwellian and consistent with the assumed boundary condition .And at altitude 2.5R_E non-Maxwellian.

However ,as altitude increase at 3.5 R_E $f(O^+)$ develops conic features distribution, because geomagnetic field strength decreases with altitude, thus the adiabatic motion of the O^+ ion drifting to higher altitudes transforms the heated distribution into one that is more geomagnetic field aligned i.e. a conic [change,1993] and the formation of ion conic is due to the combined effects of WPI, which heats the ions in the perpendicular direction and to the mirror force, which converts some of the energy gained in the perpendicular direction over to the parallel direction.

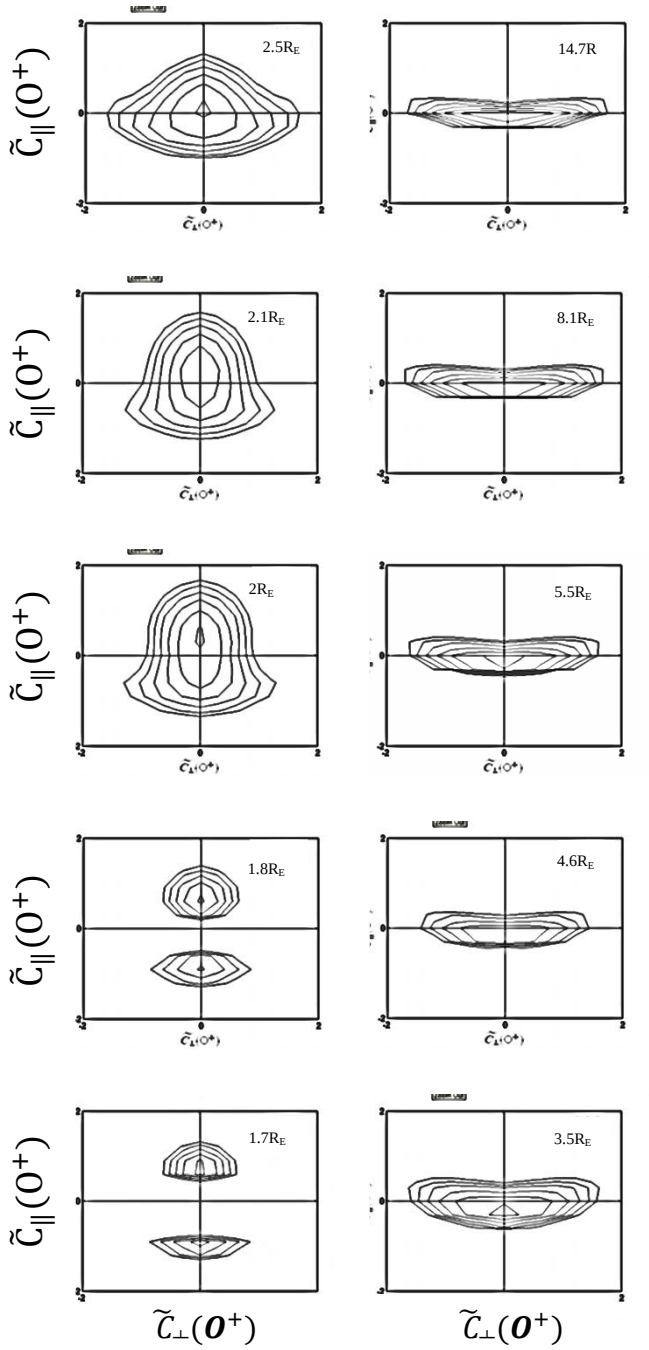

Figure (3.1): O^+ ion velocity distribution function at different geocentric distance for altitude dependent and WPI in the central polar cap region, the wave lengths. $f(O^+)$is represented by equal value contours in the normalized Velocity ($\tilde{c}_{\parallel}$,$\tilde{c}_{\perp}$) plane ,where $\tilde{c}_{\parallel} = [v - u(O^+)]/\,[2kT(O^+)/\,m(O^+)]^{1/2}$The contour levels decrease successively by a factor of $e^{1/2}$ from the maximum.

In addition we see in fig (3.2) the altitude profiles of lower order moments of O^+ ions ,which include, density $n(O^+)$, drift velocity $u(O^+)$, parallel temperature $T_{\|}(O^+)$, perpendicular temperature $T_{\perp}(O^+)$ for altitude dependent and WPI.

The drift velocity of O^+ ions $u(O^+)$ (top right panel of fig (3.2)) increases with altitude, which can be explained as follow: the effect of WPI heating the ion s in the perpendicular direction , which increase the upward mirror force ,and so increases the acceleration of the ions in the upward direction i.e. ions u(O+) increases with altitude .

The WPI (i.e. perpendicular heating) has two opposing effects on the O^+ ions density $n(O^+)$. It increases the number of O^+ ions that can escape and crossing the potential barrier and to higher altitudes , this slightly dominates at low altitudes, in constant , WIP increase the drift velocity of O^+ ions, which reduce the density of O^+ ion, this effect dominates at high altitudes (this explain the slight increase in density at low altitude and large decrease at high altitudes .

The (bottom left panel) of Fig(3.2) The behavior of this $T_{\perp}(O^+)$ is due to the effect of WPI that heats O^+ ions in the perpendicular direction, and to the effect of perpendicular adiabatic cooling, in which part of the energy is transferred from perpendicular direction to the parallel direction in order to keep the first adiabatic invariant μ constant ($\mu = mv_{\perp}^2/2B$). As altitude increases, $T_{\perp}(O^+)$ increases due to the effect of WPI that dominates the effect of perpendicular adiabatic cooling, which results from the temporary trapping of O^+ ions between the lower magnetic deflection point and the upper gravitational point when an ion bounces between these deflection points, it is accelerated in the perpendicular direction (i.e. the ion energized to higher perpendicular temperature).

The bottom right panel of Fig(3.2) This profiles of O^+ ions parallel temperature $T\|(O^+)$ is influenced by WPI, because as O^+ ions perpendicular temperature increases due to WPI, part of this energy is transferred from the perpendicular direction to the parallel direction, and consequently, the parallel temperature increases at high altitudes. At low altitudes O^+ ions parallel temperature $T_{\|}(O^+)$ decreases, owing to parallel adiabatic cooling [Barakat and Lemaire, 1990].

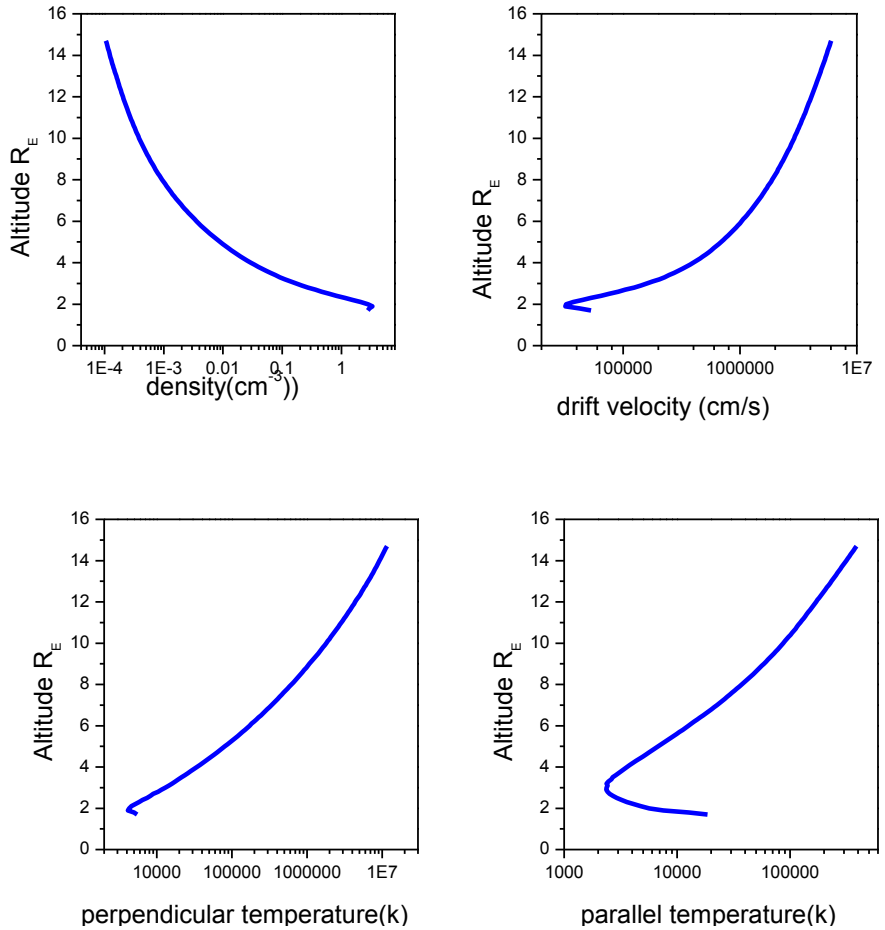

Figure (3.2):altitude profiles of the lower order O^+ moment for altitude dependent and WPI in the central polar cap region .The O^+ moments considered here are : -Density $n(O^+)$ (top left), drift velocity $u(O^+)$ (top right),perpendicular temperature $T_\perp(O^+)$(bottom left),and parallel temperature $T_\parallel (O^+)$ (bottom right).

(3.2.b) H^+ ion :

To study the effect of altitude dependent and-WPI on the H^+ ion in the central polar cap , we computed the distribution function $f(H^+)$ at several altitudes extended from 1.7 to 14.7 R_E

In Fig (3.3) presents contour plots for H^+ velocity distribution at different altitude,

At the exobase 1.7 R_E is Maxwellian which is the same as initial boundary conditions. However, as altitude increases, the distribution function develops conic features and these features saturate at higher altitudes.

The formation of ion conic is due to the combined effects of WPI, which heats the ions in the perpendicular direction and to the mirror force, which converts some of the energy gained in the perpendicular direction over to the parallel direction.

Figure (3.4) shows the profiles of H^+. Including the WPI the drift velocity u(H^+) (top right panel). which can be explained as follows, the WPI heat the ions in the perpendicular direction, which increases the upward mirror force and hence, accelerates the H^+ ions in the upward direction .

A corresponding decrease in the H^+ density n(H^+) (top left panel) is expected in order to compensate for the increase in u(H^+), there by keeping the net escape flux constant .

The behavior of the perpendicular temperature $T_\perp$ (H^+) (bottom left panel) perpendicular temperature increasing with altitude, is a result of the heating process due to WPI, of the altitude dependent and WPI, the transverse heating due to WPI dominates the perpendicular adiabatic cooling at most altitudes, Only at very low altitude, the perpendicular cooling dominates the perpendicular heating .

The bottom right panel of fig (3.4) this profiles of H^+ parallel temperature $T_\parallel$(H^+) .the behavior of $T_\parallel$(H^+) is decreasing below 2.2R_E and increasing above altitude 2.2R_E ,this is due to the balance between two effects firstly, the perpendicular heating increases the upward mirror force, and consequently, the parallel adiabatic cooling is strengthened [Barghouthi et al.,1998]. Secondly, as the ions drift upward along diverging geomagnetic field lines, $T_\parallel$(H^+) increasing due to the energy transfer from perpendicular direction over to the parallel direction.

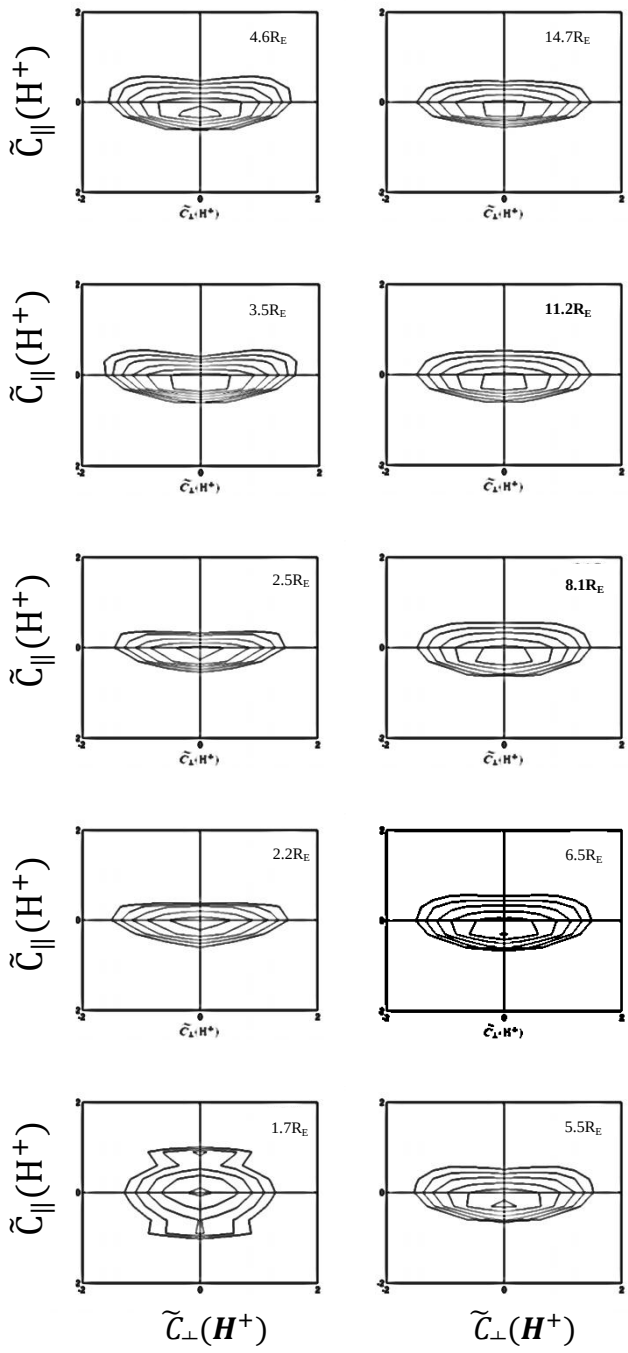

Figure (3.3): H^+ ion velocity distribution function at different geocentric distance for altitude dependent and WPI in the central polar cap region. $f(H^+)$ is represented by equal value contours in the normalized Velocity ($\tilde{c}_{\parallel}$,$\tilde{c}_{\perp}$) plane, where $\tilde{c}_{\parallel} = [v - u(H^+)]/\,[2kT(H^+)/m(H^+)]^{1/2}$ The contour levels decrease successively by a factor for $e^{1/2}$ from the maximum.

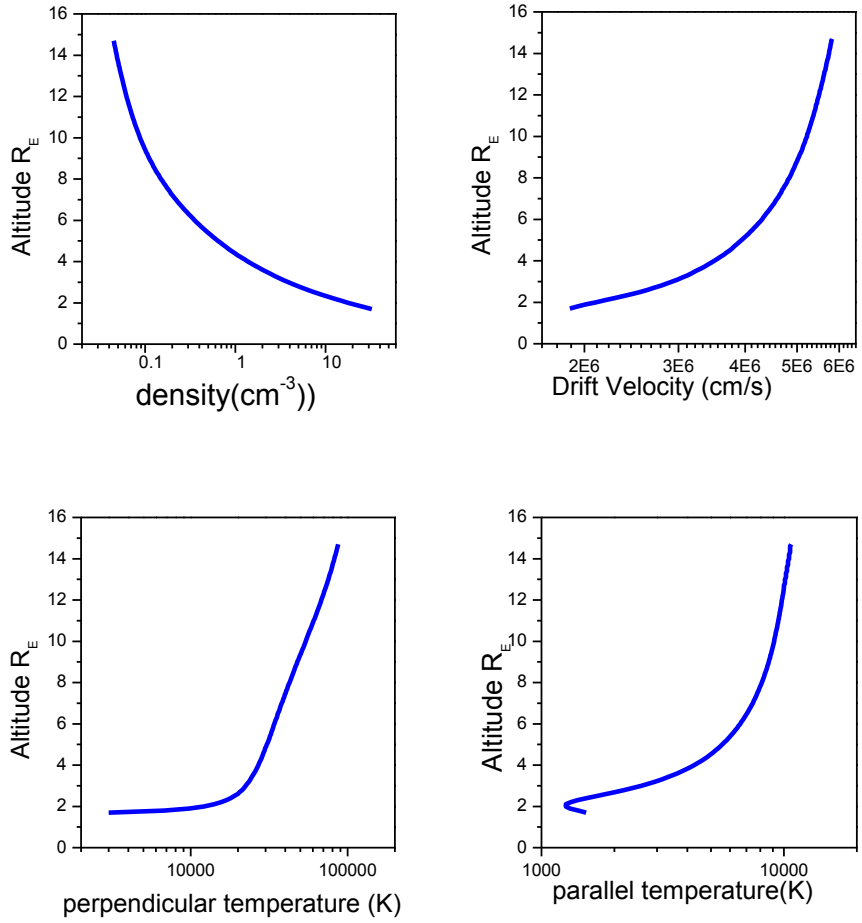

Figure (3.4): altitude profiles of the lower order H^+ moment for altitude dependent and WPI in the central polar cap region. The H^+ moments considered here are : -Density $n(H^+)$ (top left), drift velocity $u(H^+)$ (top right), perpendicular temperature $T_\perp(H^+)$(bottom left), and parallel temperature $T_\parallel$ (H^+) (bottom right).

(3.3) The results in the cusp region:

(3.3.a) O^+ ions:

Fig (3.5) presents contour plots for O^+ velocity distribution at different altitude dependent and WPI in the cusp region.

Fig (3.5) presents the contour plots of the O^+ ion velocity distribution function in the cusp region (right panel) at the exobase 1.7 R_E is half–Maxwellian which is the same as initial boundary condition. and at altitude 1.8 R_E is Maxwellian ,the conic features appeared at altitude above (~5.5R_E)

The formation of ion conic is due to the combined effects of WPI, which heats the ions in the perpendicular direction and to the mirror force, which converts some of the energy gained in the perpendicular direction over to the parallel direction.

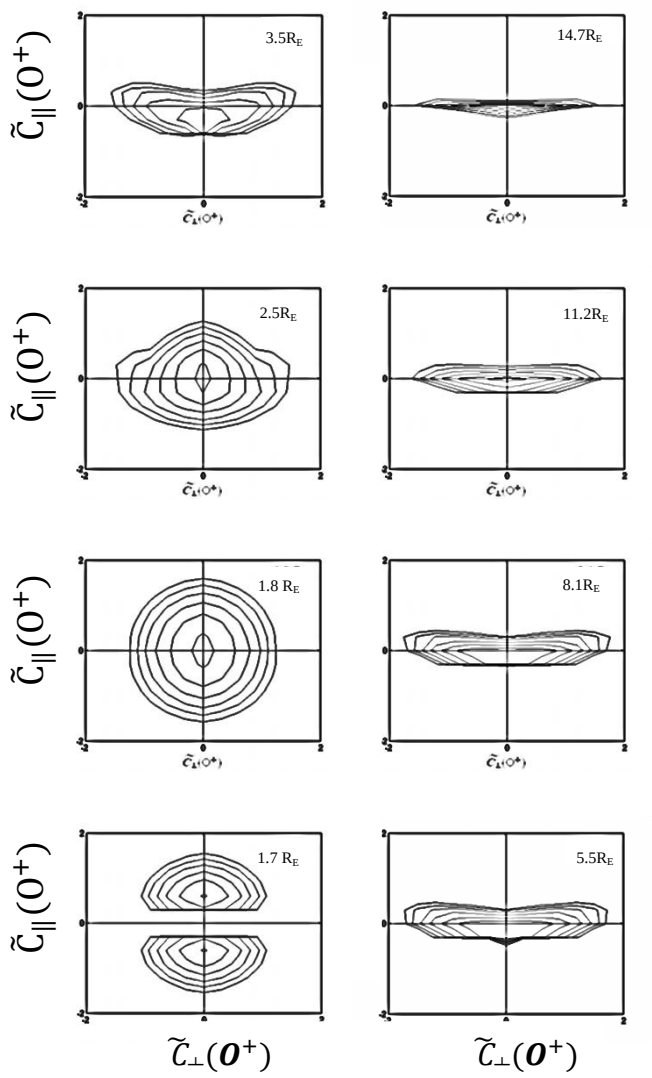

Figure (3.5): O^+ ion velocity distribution function at different geocentric distance for altitude dependent and WPI in the cusp region . $f(O^+)$is represented by equal value contours in the normalized Velocity $(\tilde{c}_{\parallel},\tilde{c}_{\perp})$,where $\tilde{c}_{\parallel} = [v - u(O^+)]/\,[2kT(O^+)/m(O^+)]^{1/2}$ The contour levels decrease successively by a factor for $e^{1/2}$ from the maximum.

In addition we see in fig (3.6) the altitude profiles of lower order moments of O^+ ions, which include, (density $n(O^+)$, drift velocity $u(O^+)$, parallel temperature $T_{\parallel}(O^+)$, perpendicular temperature $T_{\perp}(O^+)$ for altitude dependent and WPI.

The drift velocity of O^+ ions u(O^+) (top right panel of fig (3.6) increases with altitude, which can be explained as follow, the effect of WPI heating the ion s in the perpendicular direction, which increases the upward mirror force, and so increases the acceleration of the ions in the upward direction i.e. ions u(O+) increases with altitude .

The WPI (i.e. perpendicular heating) has two opposing effects on the O^+ ions density n(O^+).it increases the number of O^+ ions that can escape and crossing the potential barrier and to higher altitudes, this slightly dominates at low altitudes in constant, WIP increase the drift velocity of O^+ ions, which reduce the density of O^+ ion, this effect dominates at high altitudes (this explain the slight increases in density at low altitude and large decrease at high altitudes.

The (lower left panel) of Fig(3.6) The behavior of this $T_\perp(O^+)$ is due to the effect of WPI that heats O^+ ions in the perpendicular direction, and to the effect of perpendicular adiabatic cooling, in which part of the energy is transferred from perpendicular direction to the parallel direction in order to keep the first adiabatic invariant μ constant (i.e.$\mu = mv_\perp^2/2B$) . As altitude increases, $T_\perp$ (O^+) increases due to the effect of WPI that dominates the effect of perpendicular adiabatic cooling, which results from the temporary trapping of O^+ ions between the lower magnetic deflection point and the upper gravitational point when an ion bounces between these deflection points, it is accelerated in the perpendicular direction (i.e. the ion energized to higher perpendicular temperature).

The (lower right panel) of Fig(3.6) This profiles of O^+ ions parallel temperature $T_\parallel(O^+)$ is influenced by WPI, because as O^+ ions perpendicular temperature increases due to WPI, part of this energy is transferred from the perpendicular direction to the parallel direction, and consequently, the parallel temperature increases at high altitudes. At low altitudes O^+ ions parallel temperature $T_\parallel$ (O^+) decreases, owing to parallel adiabatic cooling [Barakat and Lemaire, 1990].In the parallel temperature in cusp region is the decreasing below 2.2R_E and increasing above altitude 2.2 R_E .

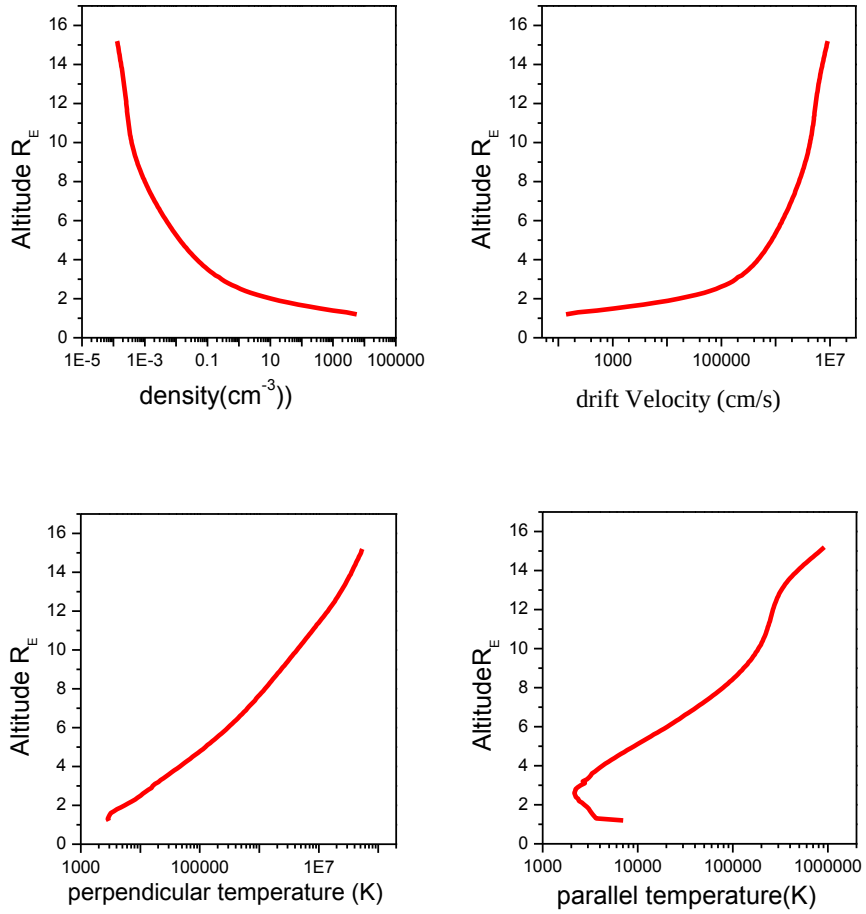

Fig (3.6): altitude profiles of the lower order O^+ moment for altitude dependent and WPI in the cusp region. The O^+ moments considered here are : -Density $n(O^+)$ (top left), drift velocity $u(O^+)$ (top right), perpendicular temperature $T\perp(O^+)$(bottom left), and parallel temperature $T_{\|}$ (O^+) (bottom right).

(3.3.b) H^+ ions:

Fig (3.7) presents contour plots for H^+ velocity distribution at different altitude dependent WPI in the cusp region.

In the cusp region, The behavior of H^+ ions is half – Maxwellian at ($1.7R_E$), and starts conic features at altitude above $2R_E$.

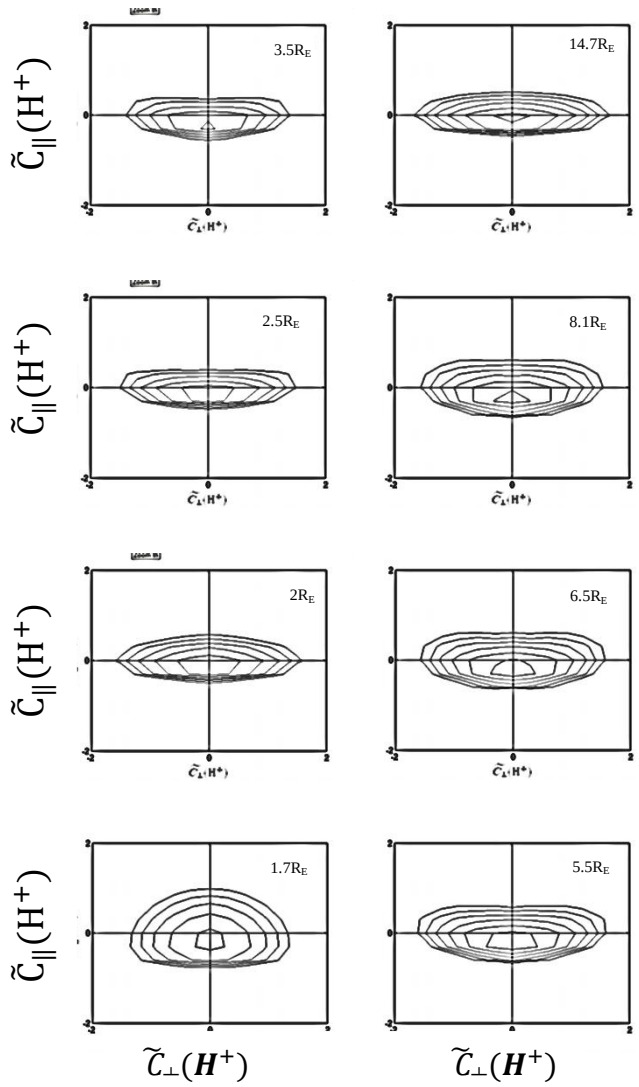

Figure (3.7):H^+ ion velocity distribution function at different geocentric distances in the cusp region. $f(H^+)$ is represented by equal value contours in the normalized Velocity $(\tilde{c}_{\parallel},\tilde{c}_{\perp})$,where $\tilde{c}_{\parallel} = [v - u(H^+)]/\,[2kT(H^+)/m(H^+)]^{1/2}$The contour levels decrease successively by a factor for $e^{1/2}$ from the maximum.

In addition we see in fig (3.8) the altitude profiles of lower order moments of H^+ ions ,which include, density $n(H^+)$, drift velocity $u(H^+)$, parallel temperature $T_{\parallel}(H^+)$, perpendicular temperature $T_{\perp}(H^+)$ for altitude dependent WPI.

Figure (3.8) shows the profiles of H^+. Including the WPI the drift velocity $u(H^+)$ (top right panel). which can be explained as follows, the WPI heat the ions in the perpendicular direction, which increases the upward mirror force and hence, accelerates the H^+ ions in the upward direction .

A corresponding decrease in the H^+ density $n(H^+)$ (top left panel) is expected in order to compensate for the increase in $u(H^+)$, thereby keeping the net escape flux constant .

The behavior of the perpendicular temperature $T\perp(H^+)$ (bottom left panel) perpendicular temperature increasing with altitude, is a result of the heating process due to WPI, of the altitude dependent and WPI, the transverse heating due to WPI dominates the perpendicular adiabatic cooling at most altitudes, Only at very low altitude, the perpendicular cooling dominates the perpendicular heating .

The profile s of H^+ parallel temperatures $T_{\|}(H^+)$ is presented in (bottom right panel) of fig (3.8). The behavior of $T_{\|}(H^+)$ is decreasing below $2.2R_E$ and increasing above altitude $2.2R_E$, this is due to the balance between two effects. Firstly, the perpendicular heating increases the upward mirror force, and consequently, the parallel adiabatic cooling is strengthened [Barghouthi et al.,1998] . Secondly, as the ions drift upward along diverging geomagnetic field lines, $T_{\|}(H^+)$ increasing due to the energy transfer from perpendicular direction over to the parallel direction .

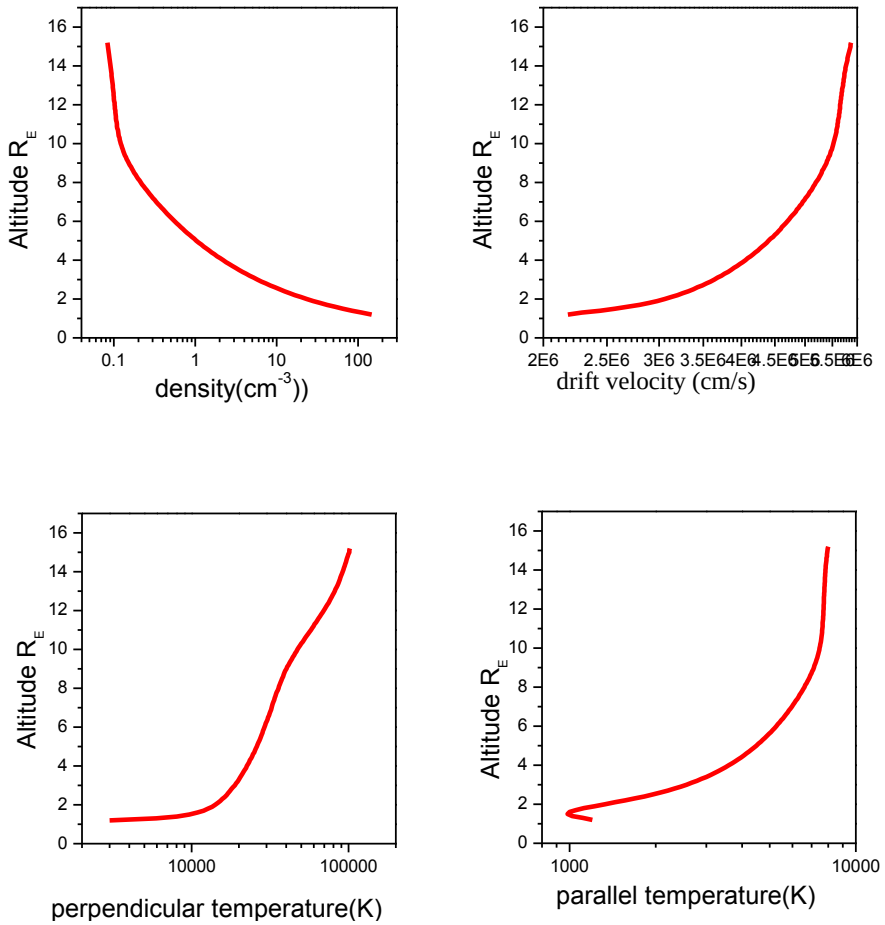

Fig (3.8):altitude profiles of the lower order H^+ moment for altitude WPIin the cusp region .The H^+ moments considered here are : -Density $n(H^+)$ (top left), drift velocity $u(H^+)$ (top right),perpendicular temperature $T\perp(H^+)$(bottom left),and parallel temperature $T_{\parallel}(H^+)$ (bottom right).

Chapter Four

Comparisons and Conclusions

Chapter four

Comparisons and conclusions

(4.1) Comparisons and conclusions:

In this chapter, we are going to compare between the simulation results for both ions (H^+ and O^+) in both regions (central polar cap and cusp), by using two different diffusion coefficients. Diffusion coefficients obtained from Dynamics Explorer 1spacecraft [Barghouthi 1997, and Barghouthi et al 1998] and diffusion coefficients obtained from cluster space craft [Nilsson et al 2012, 2013]. These coefficients are given in the following equations:

Barghouthi coefficients:

$$D_{\perp} = 9.55 * 10^2 \left(\frac{r}{R_E}\right)^{13.3} [cm^2 s^{-3}] \quad \ldots\ldots\ldots\ldots\ldots\ldots \quad central\ polar\ cap\ for\ O^+$$

$$D_{\perp} = 5.77 * 10^3 \left(\frac{r}{R_E}\right)^{7.95} [cm^2 s^{-3}] \quad \ldots\ldots\ldots\ldots\ldots central\ polar\ cap for\ H^+$$

$$D_{\perp} = 6.94 * 10^5 \left(\frac{r}{R_E}\right)^{13.3} [cm^2 s^{-3}] \ \ldots\ldots\ldots\ldots\ldots\ldots\ldots\ldots\ldots\ldots cusp\ for\ O^+$$

$$D_{\perp} = 4.45 * 10^7 \left(\frac{r}{R_E}\right)^{7.95} [cm^2 s^{-3}] \ldots\ldots\ldots\ldots\ldots\ldots\ldots\ldots\ cusp\ for\ H^+$$

Nilsson coefficients

$$D_{\perp} = \eta * 10 * \left(\frac{r}{R_E}\right)^{5.5} [cm^2 s^{-3}] \quad \ldots\ldots\ldots\ldots\ldots \quad central\ polar\ cap\ for\ O^+$$

$$D_{\perp} = \eta\ (2.3) * 10^6 [cm^2 s^{-3}] \ldots\ldots\ldots\ldots\ldots central\ polar\ cap for\ H^+$$

$$D_{\perp} = \eta\ 1725 \left(\frac{r}{R_E}\right)^{3.3} [cm^2 s^{-3}] \ldots\ldots\ldots\ldots\ldots\ldots\ldots\ldots\ldots\ldots cusp\ for\ O^+$$

$$D_{\perp} = \eta\ (2.3)(10^6)\ [cm^2 s^{-3}] \ldots\ldots\ldots\ldots\ldots\ldots\ldots\ldots\ cusp\ for\ H^+$$

The altitude behavior of these diffusion coefficients is shown in figure (4.1).

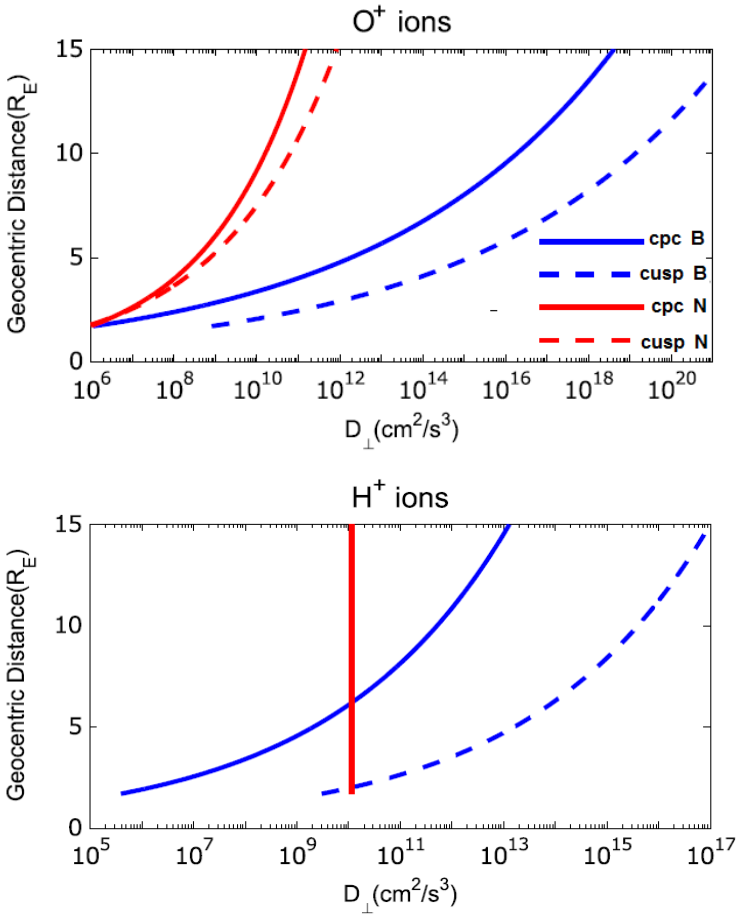

Figure (4.1): Profiles of the perpendicular diffusion coefficients (Barghouthi) and (Nilsson) in central polar cap and cusp regions (top panel) $D_{\perp}$ (O^{+}) and (bottom panel) $D_{\perp}$ (H^{+}) for different altitudes**.**

In the following figures (4.2, 4.3. 4.4, 4.5, 4.6, and 4.7) we are going to present the comparison and to comment on the comparison itself, because the physics of the altitude behavior for each ion outflow has been discussed either in previous chapter or in [Barghouthi 1997 and Barghouthi et al., 1998].

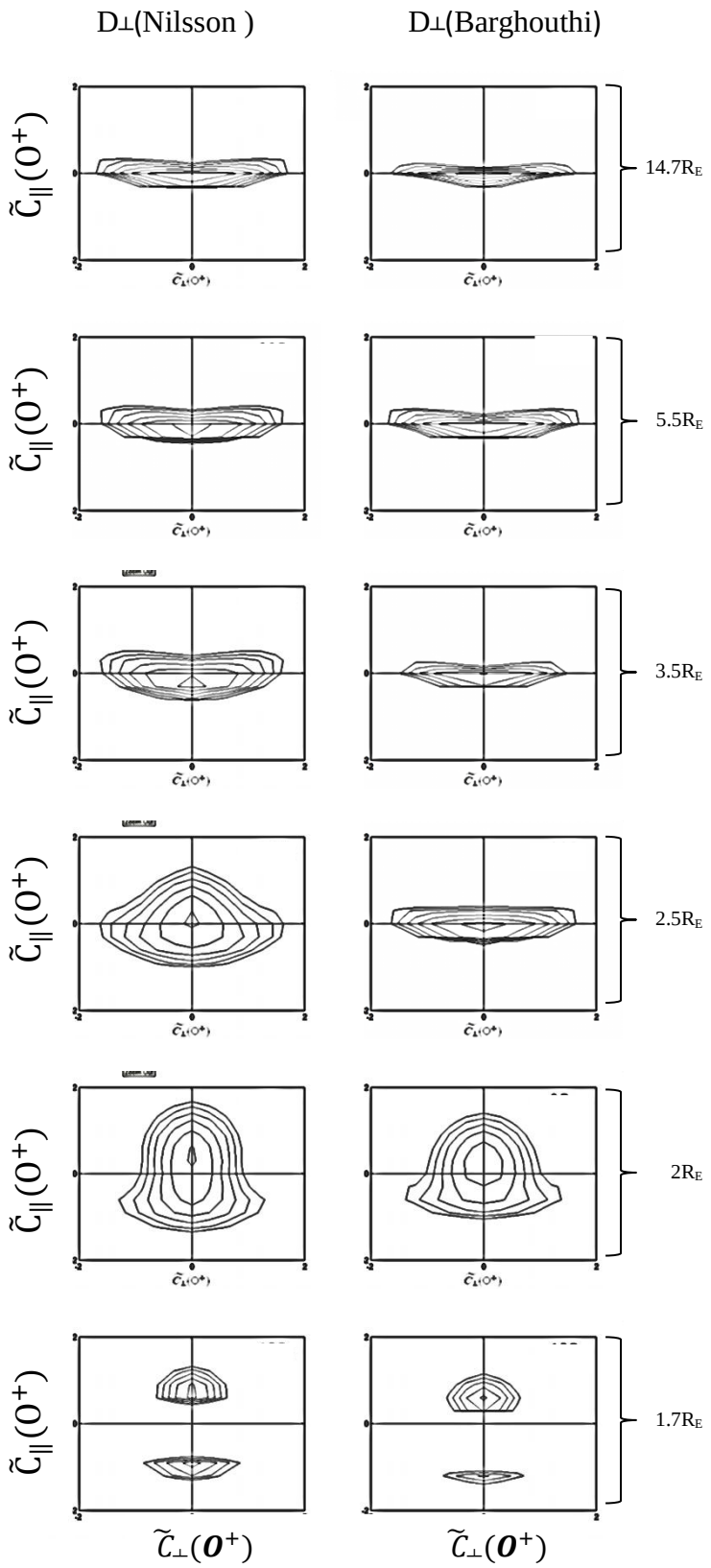

Figure(4.2) :O^+ ions distribution at different geocentric altitude in the central polar cap regions by using D⊥ (Nilsson) left panel and D⊥ (Barghouthi) right panel . f (O^+) is represented by equal

value contours in the normalized velocity $(\tilde{c}_{\parallel},\tilde{c}_{\parallel})$ plane, where $\tilde{c}_{\parallel} = [v - u(O^+)]/\,[2kT(O^+)/ m(O^+)]^{1/2}$The contour levels decrease successively by afactor for $e^{1/2}$ from the maximum.

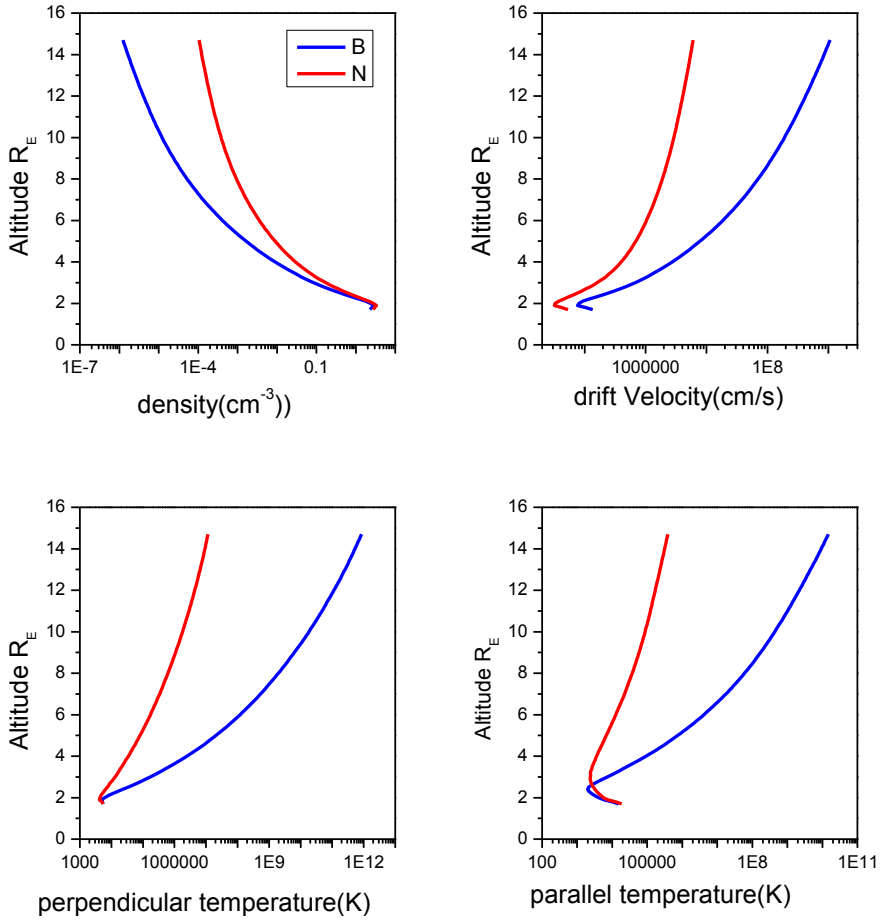

Fig (4.3): altitude profiles of the lower order O^+ moment for central polar cap regions by using D⊥(Nilsson)(red–solid)and D⊥ (Barghouthi) (blue-solid). the moments considered here are:- density n(cm^{-3})(top left), drift velocity u(cm/s)(top right), perpendicular temperature T⊥(k) (bottom left), and parallel temperature $T_{\parallel}$(k) (bottom right).

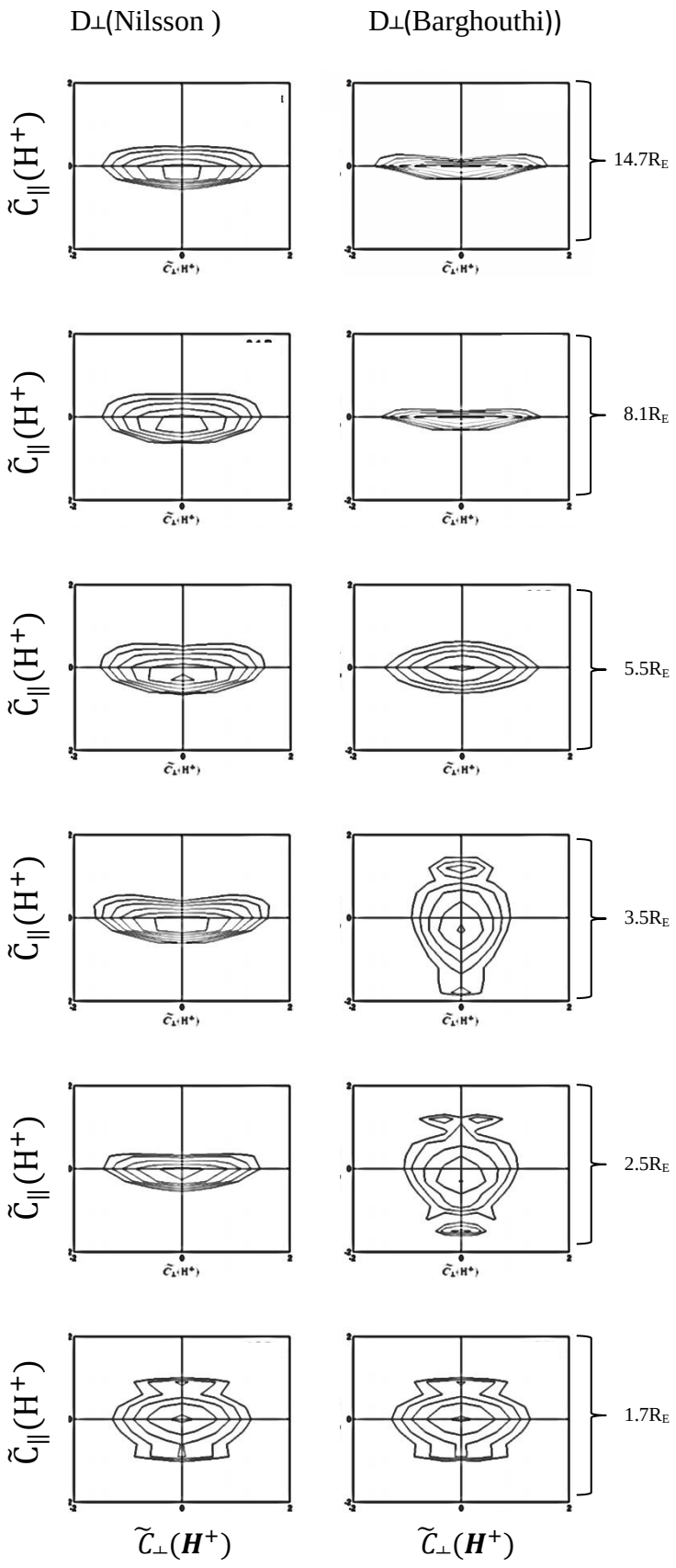
D⊥(Nilsson)
D⊥(Barghouthi))
$\tilde{C}_{\parallel}(H^+)$
14.7R_E
8.1R_E
5.5R_E
3.5R_E
2.5R_E
1.7R_E
$\tilde{C}_{\perp}(H^+)$
$\tilde{C}_{\perp}(H^+)$

Fig(4.4) : H^+ ions distribution at different geocentric altitudes in the central polar cap regions by using D⊥ (Nilsson)left panel and D⊥ (Barghouthi) right panel. f(H^+) is represented by equal value contours in the normalized velocity ($\tilde{c}_{\|}$,$\tilde{c}_{\|}$) plane ,where $\tilde{c}_{\|} = [v - u(H^+)]/\,[2kT(H^+)/\, m(H^+)]^{1/2}$The contour levels decrease successively by afactor for $e^{1/2}$ from the maximum.

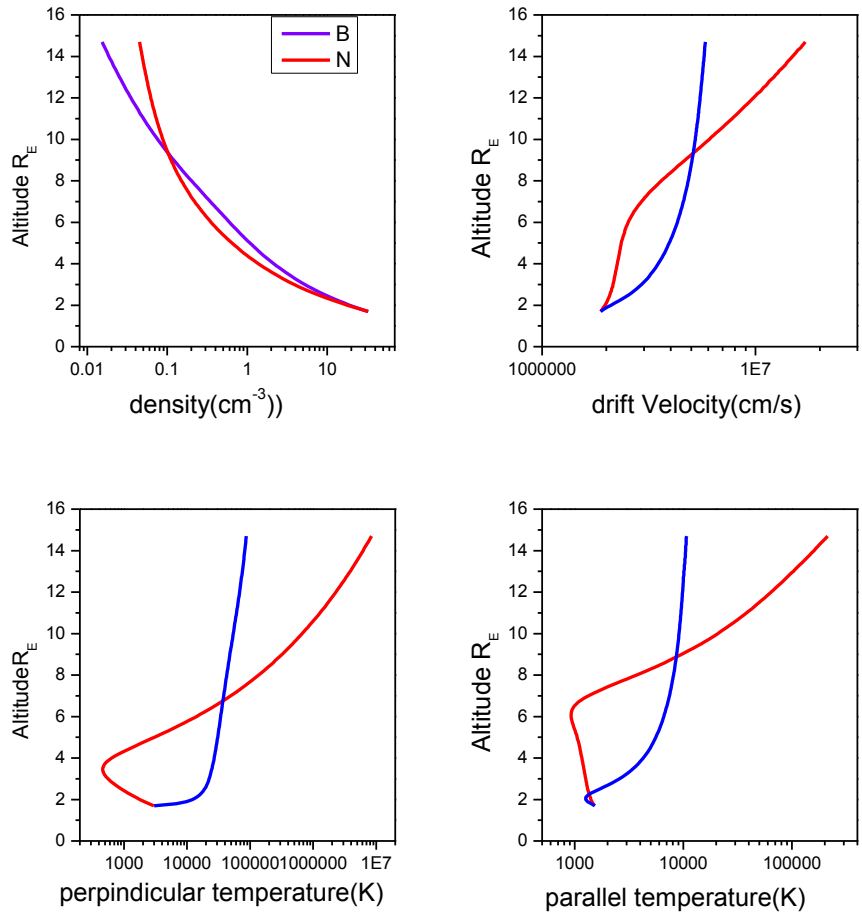

Figure (4.5): altitude profiles of the lower order H^+ moments for central polar cap regions by using D⊥(Nilsson)(red–solid) and D⊥(Barghouthi)(blue-solid). The moments considered here are: density n(cm^{-3})(top left), drift velocity u(cm/s)(top right)perpendicular temperature T⊥(k)(bottom left) , and parallel temperature $T_{\|}$(k)(bottom right).

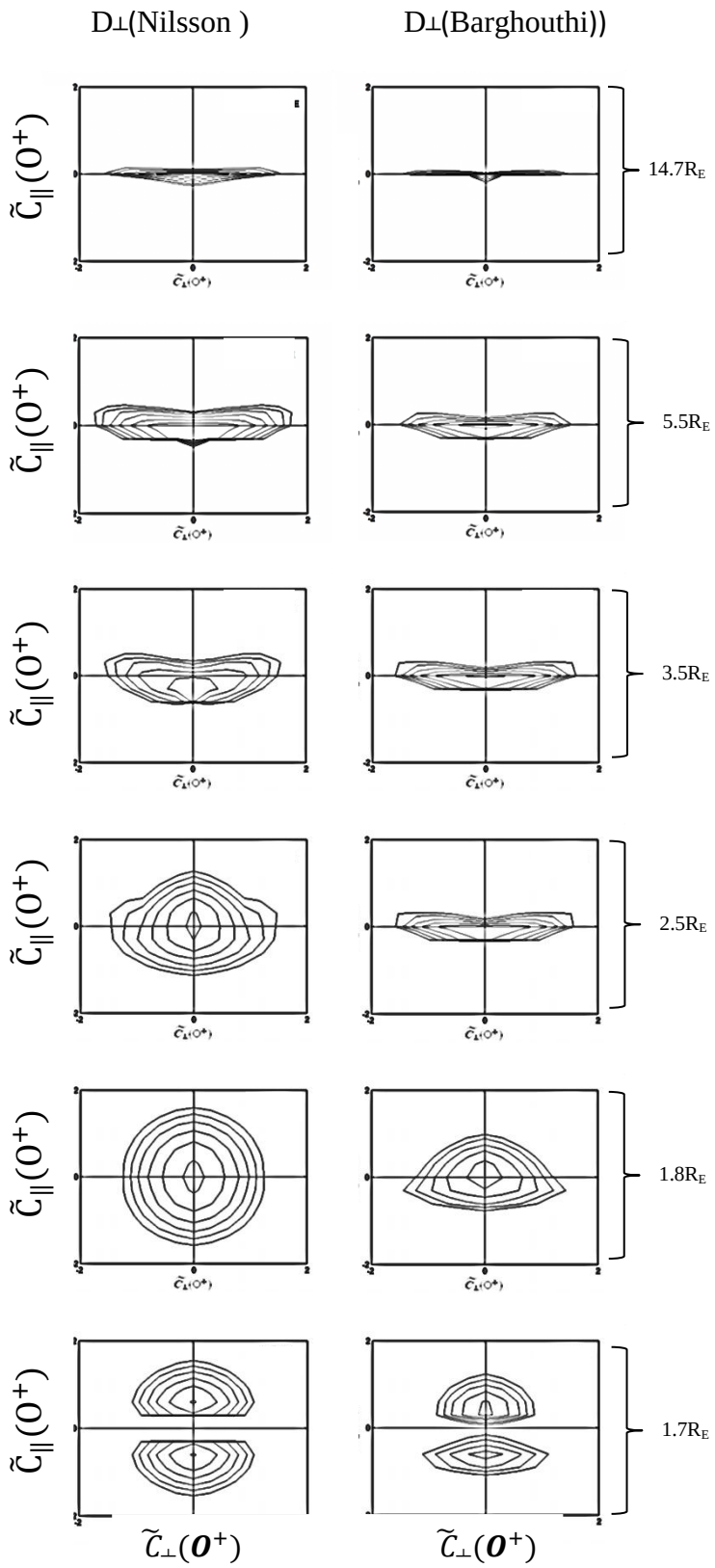

Fig(4.6): O^+ ions velocity distribution function at different geocentric altitudes in the cusp regions by using D⊥ (Nilsson)left panel and D⊥ (Barghouthi) right panel. f(O^+) is represented by equal

value contours in the normalized velocity $(\tilde{c}_{\parallel},\tilde{c}_{\parallel})$ plane ,where $\tilde{c}_{\parallel} = [v - u(O^+)]/\,[2kT(O^+)/ m(O^+)]^{1/2}$The contour levels decrease successively by afactor for $e^{1/2}$ from the maximum.

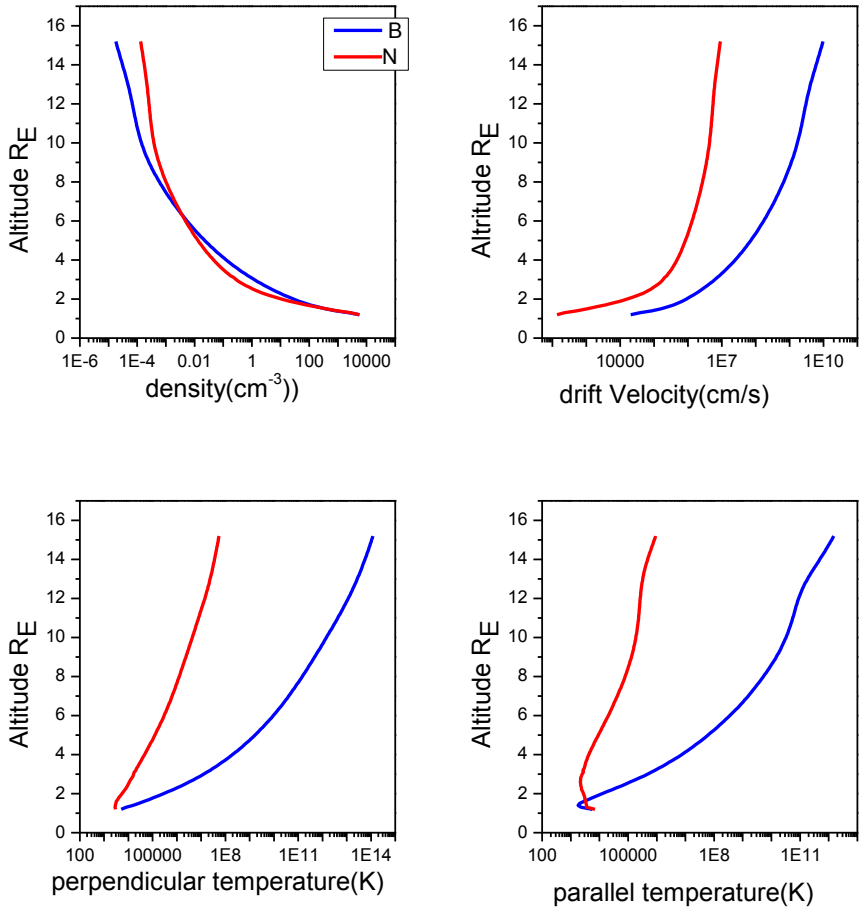

Fig (4.7): altitude profiles of the lower order O^+ moments for cusp regions by using $D_\perp$ (Nilsson) (red – solid) and $D_\perp$ (Barghouthi) (blue-solid). the moments considered here are: density n(cm^{-3})(top left), drift velocity u (cm/s)(top right) perpendicular temperature $T_\perp$(k) (bottom left) , and parallel temperature $T_\parallel$(k)(bottom right).

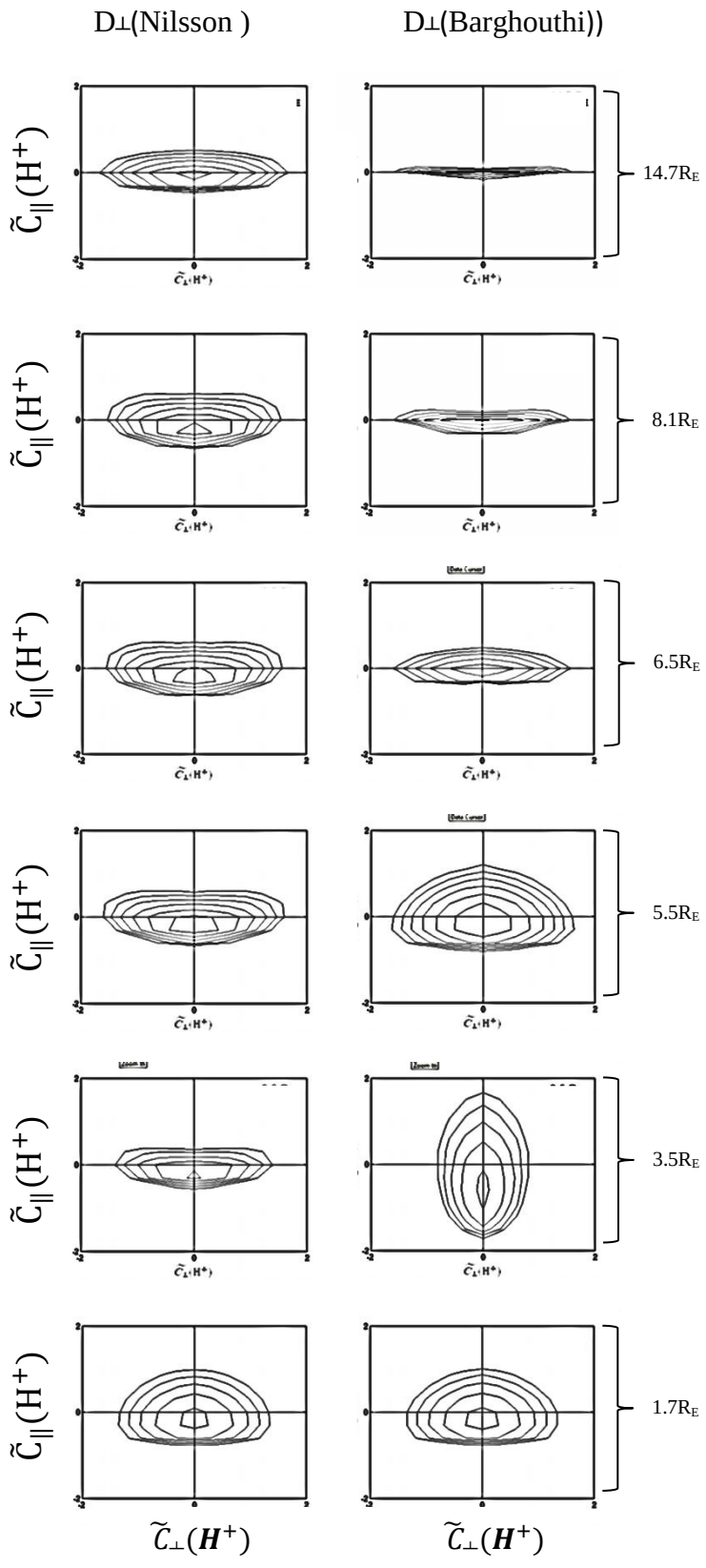

Figure (4.8): H^+ ions velocity distribution function at different altitudes in the cusp regions by using D⊥ (Nilsson)left panel and D⊥ (Barghouthi) right panel . f(H^+) is represented by equal value

contours in the normalized velocity ($\tilde{c}_{\parallel}$,$\tilde{c}_{\parallel}$) plane, where $\tilde{c}_{\parallel} = [v - u(H^+)]/\,[2kT(H^+)/ m(H^+)]^{1/2}$The contour levels decrease successively by afactor for $e^{1/2}$ from the maximum.

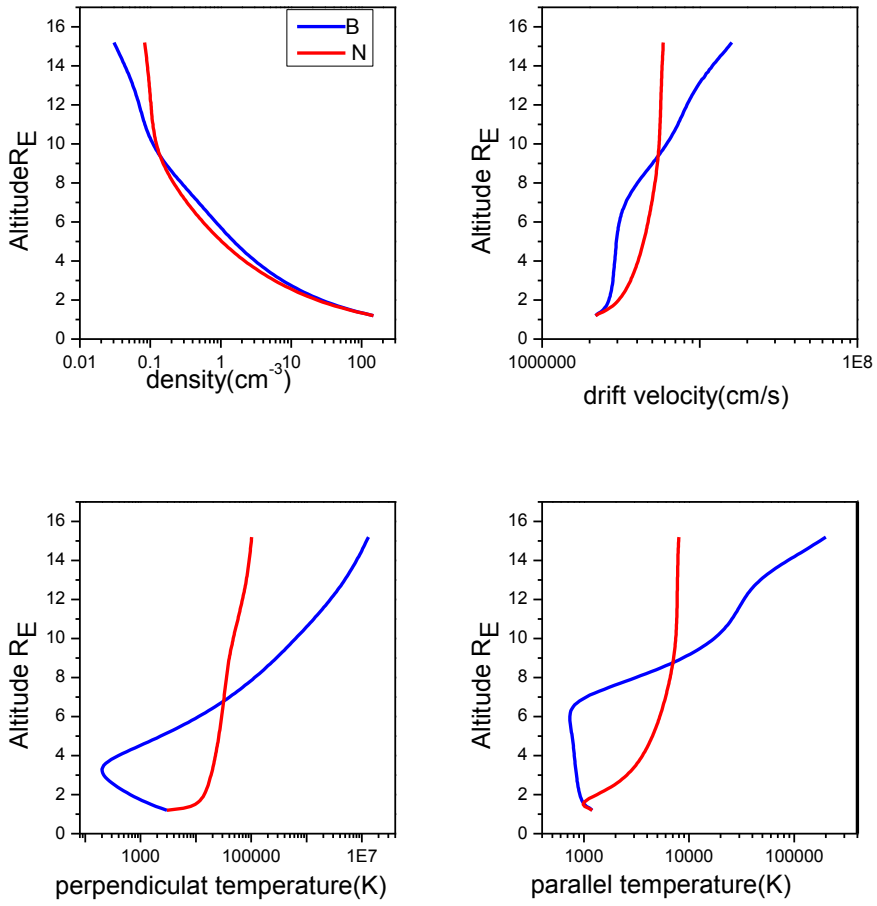

Fig (4.9): altitude profiles of the lower order H^+ moments for cusp regions by using $D_{\perp}$ (Nilsson) (red –solid) and $D_{\perp}$ (Barghouthi) (blue-solid). the moments considered here are :density n(cm^{-3}) (top left), drift velocity u (cm/s) (top right), parallel temperature $T_{\parallel}$(k) (bottom right), and Perpendicular temperature $T_{\perp}$ (k) (bottom left).

It is very obvious that there is a big difference between both simulation results due to different diffusion coefficients; this difference is attributed to the behavior of the diffusion coefficient. According to the altitude behavior of the diffusion coefficients shown in figure 4.1, we can say that the numerical values due to DE-1 satellite are much higher than the corresponding values due to Cluster spacecraft. These discrepancies are due to the orbit of the satellite and to different geophysical conditions. The orbit of DE-1 satellite is between 1.7 and 4.6 R_E and the orbit of the Cluster is between 5.6 and 16 R_E. In order to cover the whole simulation tube, Barghouthi has to extrapolate the diffusion coefficients at higher altitudes, and Nilsson has to extrapolate the diffusion coefficients in the lower altitudes. Currently, Hamza Abudayyaeh (graduate student, al-Quds university) Barghouthi, Nilsson ,and Slapak are working to remove this discrepancy by choosing appropriate observations and corresponding diffusion coefficients.

References

Abe, T.,Whalen,B.A.,Yau, A. W., Horita, R. E.,Watanbe S., and Sagawa, E.: EXOS D (Akebono) Suprathermal mass spectrometer observations of the polar wind, J. Geophys. Res., 98, 11, 191, 1993.

Aldrich C., Paiticle code simulations with injected particles, space science reviews, 42, 131,1985.

Arvelius, S., Statistics of high-altitude and high-latitude O+ ion outflows observed by Cluster/CIS, Ann. Geophys., 23, 1909–1916, 2005.

Axford ,W., the polar wind and the terrestrial helium budeget, J. geophys. Res., 73,6855, 1968.

Band electromagnetic turbulence,Phys.Rev.lett, doi:10.1103/PhysRevlett.59, 148,1987.

Banks, P.M. and Holzer, T.E.: The polar wind, J. Geophys. Res. **73**, 6846, 1968.

Banks, P.M., and T. E. Holzer, High-latitude plasma transport: The polar wind, J. Geophys .Res.,7 4, 6317-6332,1 969.

Banks,P .M., and T. E. Holzer, Featureso f plasmat ransporitn the upper atmosphere, J. Geophys.R.es.,7 4, 630z•6316,1 969.

Barakat, A. and R. Schunk, Comparison of Maxwellian and bi-Maxwellian expansions with Monte Carlo simulations for anisotropic plasmas, J. Phys. D, 15, 2189, 1982C.

Barakat, A. R., and Barghouthi, I. A.: The effects of wave-particle interactions on the polar wind O^+, Geophys. Res. Lett., 21 2279-2282, 1994a.

Barakat, A. R., and Barghouthi, I. A.: The effects of wave-particle interactions on the polar wind: Preliminary results, Planet. Space Sci., 42, 987-992, 1994b.

Barakat, A. R., and Lemaire, J.: Monte Carlo study of the escape of a minor species, Phys. Rev. A., 42, 3291-3302, 1990.

Barakat, A. R., and R. W. Schunk, Stability of polar wind, J. Geophys.Res., 94, 147-1494,1989.

Barakat, A. R., R. W. Schunk, and J. P. St.-Maurice, Monte Carlo calculations of the O+ velocity distribution in the auroral ionosphere,J. Geophys. Res., 88, 3237–3241(1983).

Barakat, A.R. and Schunk, R.W.: 1983, O+ ions in the polar wind, J. Geophys. Res., 88, 7887.7894,1983.

Barghouthi I. A., Barakat, A. R., and Persoon, A. M.: The effects of altitude –dependent wave particle interactions on the polar wind plasma, Astrophysics and space sciences, 259, 117, 1998

Barghouthi, I. A. :A Monte Carlo study for ion outflows at high altitude and high latitude: Barghouthi model, J. Geophys. Res., 113, A08209. 1- 11, 2008.

Barghouthi, I. A. O^+ion temperature partition coefficients $\beta_{\parallel}$ and $\beta_{\perp}$: effect of O^+- O^+ Coulomb self-collisions, J. Geophys. Res., 110, A06307. 1- 7, (2005)..

Winkler, E., J. P. St.-Maurice, and A. R. Barakat Results from improved Monte Carlo calculations of auroral ion velocity distributions,J. Geophys. Res., 97, 8399– 8423, (1992).

Barghouthi, I. A., Naji Qatanani, and Fathi Allan Monte Carlo simulation of Boltzmann equation in space plasma Monte Carlo Methods and Applications, 9 (3), 2003.

Barghouthi, I. A., S. H. Ghithan, and H. Nilsson A comparison study between observations and simulation results of Barghouthi model for O^+ and H^+outflows in the polar wind, Annales Geophysicae, 29, 2061 – 2079, 2011.

Barghouthi, I. A., and Atout, M. A.: Monte Carlo modeling of toroidal ion distributions and ion temperatures at high altitudes equatorward of the cusp: Effect of finite gyroradius, J. Geophys. Res., 111, A03202, 2006.

Barghouthi, I. A., and Barakat, A. R.: Comparison between the wave-particle interaction in the polar wind and in the auroral region, Phys. Space Plasmas, 13, 445– 450, 1995.

Barghouthi, I. A., Doudin, N. M., Saleh, A. A. ,Pierrard, V.: The effect of altitude and velocity dependent wave-particle interactions on the H^+ and O^+ outflows in the auroral region, Journal of atmospheric and solar-terrestrial physics,70, 1159 – 1169, 2008.

Barghouthi, I. A., Doudin, N. M., Saleh, A. A., and Pierrard, V.: High-altitude and high-latitude O^+ and H^+ outflows: the effect of finite electromagnetic turbulence wavelength , Ann. Geophys., 25, 2195-2202, 2007.

Barghouthi, I. A., E. I. Elias, M. A. Abu Samra, N. A. Qatanani, and M. S. Issa (2003a), Monte Carlo simulation of O+ behavior in the auroral ionosphere, J. Phys. Soc. Jpn., 72, 3006– 3013, 2003a.

Barghouthi, I. A., N. A. Qatanani, and F. M. Allan , Monte Carlo simulation of Boltzmann equation in space plasma at high latitudes, Monte Carlo Methods Appl., 9, 201– 216, 2003b .

Barghouthi, I. A.: Effects of wave particle interactions on H^+ and O^+ outflow at high latitude; A comparative study, J. Geophys. Res., 102, 22. 062-22.075, 1997.

Baure,S,J., on The structure of the topside ionosphere ,Electron Density Profiles in Ionosphere and Exosphere,edited by J.Frihagen,North-Holland,NewYork,P.387,1966.

Bellan P.M., Fundamentals of Plasma physics , 2004.

Bouhram, M., Dubouloz, N., Malingre, M., Jasperse, J. R., Pottelette, R., Senior, C., Delcourt, D., Carlson, C. W., Roth, I., Berthomier, M., and Sauvaud, J.-A.: Ion outflow and associated perpendicular heating in the cusp observed by InterballAuroral Probe and Fast Auroral Snapshot, J. Geophys. Res., 107(A2), 1023, doi:10.1029/2001JA000091, 2002.

Bouhram, M., Klecker, B., Miyake, W., R`eme, H., Sauvaud, J.- A., Malingre, M., Kistler, L., and Blˇagˇau, A.: On the altitude dependence of transversely heated O+ distributions in the cusp/cleft, Ann. Geophys., 22, 1787–1798, doi:10.5194/angeo- 22-1787-2004, 2004.

Bouhram, M., Malingre, M., Jasperse, J. R., and Dubouloz, N.: Modeling transverse heating and outflow of ionospheric ions from the dayside cusp/clef: 1 A parametric study, Ann. Geophys., 21, 1753-1771, 2003.

Bouhram, M., Malingre, M., Jasperse, J. R., and Dubouloz, N.: Modeling transverse heating and outflow of ionospheric ions from the dayside cusp/cleft. 1 A parametric study, Ann. Geophys., 21, 1753–1771, doi: 10.5194/angeo-21-1753-2003, 2003a.

Bouhram, M., Malingre, M., Jasperse, J. R., Dubouloz, N., and Sauvaud, J.-A.: Modeling transverse heating and outflow of ionospheric ions from the dayside cusp/cleft. 2 Applications,Ann. Geophys., 21, 1773–1791, doi:10.5194/angeo-21-1773,2003b.

Caroline rayner et al., Philips Astronomy encyclopedia, 2002.

Chang, T., Crew, G. B., Hershkowitz, N., Jasperse, J. R., Retterer, J. M., and Winningham, J. D.: Transverse acceleration of oxygen ions by electromagnetic ion cyclotron resonance with broadband left-hand polarized waves, J. Geophys. Res. Lett., 13, 636, 639, 1986.

Chang, T., Lower Hybrid collapse, caviton turbulence, and charged particle energization in the topside auroral ionosphere and magnetosphere, Phys. Fluids, B 5(7), 2646-2656,1993.

Crew, G.B.,T.change.Asympototic theory of ion conic distributions. Physics of fluids 28(8),2382-2394,1985.

Desseler,A.J.,andF.C.Michel,plasma in the geomagnetic tail,J.Geophys.Res., 71,1421,1966.

Gaimard, P., J.-P. St.-Maurice, C. Lathuillere, and D. Hubert ,On the improvement of analytical calculations of collisional auroral ion velocity distributions using recent Monte Carlo results, J. Geophys. Res., 103, 4079–4095, 1998.

Gurgiolo, C., Burch, J. L.: DE-1 observations of the polar wind – A heated and unheated component, Geophys. Res. Lett.,9, 945-948, 1985.

Gurnett, D. A., and U.S. Inan, Plasma wave observations with theDynamicsE xplorer1 spacecrafRt,ev.G eophys2.,6 , 285-316,1 988.

Gurnett, D.A., Huff, R.L., Menietti, J.D., Burch, J.L., Winningham, J.D. and Shawhan, S.D: Correlated low-frequency electric and magnetic noise along the auroral field lines, J. Geophys. Res. **89**, 8971–8985, 1984.

Hubert, D., and A. R. Barakat , Comparison of Monte Carlo simulation and polynomial expansions of auroral Non-Maxwellian distributions, 1, The 3-D representation, Ann. Geophys., 8, 687– 696,1990.

Huddleston, M. M., C. J. Pollock, M. P. Wuest, J. S. Pichett, T. E. Moore, and W. K. Peterson, Toroidal ion distributions observed at high altitudes equatorward of the cusp, Geophys. Res. Lett., 27(4), 469-472, 2000.

Korth, A.; The structure of high altitude O+ energization and outflow; A case study, Ann. Geophys., 2497-2506., 2004.

Nilsson, H., An assessment of the role of the centrifugal acceleration mechanism in high altitude polar cap oxygen ion outflow, Ann. Geophys., 26, 145–157, 2008a.

Nilsson, H., Joko, S., Lundin, R., Rème, H., Sauvaud, J.-A., Dandouras, I., Balogh, A., Carr, C., Kistler, L. M., Klecker, B., Carlson, C. W., Bavassano-Cattaneo, M, 2003b.

Nilsson, H., The structure of high altitude O+ energization and out flow: A case study, Ann. Geophys., 22, 2497– 2506.2003a.

Nilsson, H., Waara, M., Marghitu, O., Yamauchi, M., Lundin, R., Rème, H., Sauvaud, J.-A., Dandouras, I., Lucek, E., Kistler, L. M., Klecker, B., Carlsson, C. W., Bavassano-Cattaneo, M.

B. and Korth, A.; Transients in oxygen outflow above the polar cap as observed by the Cluster spacecraft, Ann. Geophys., 26, 3365-3373, 2008.

Nilsson, N., I. A. Barghouthi, R. Slapak, A. I. Eriksson, and M. André , Hot and cold ion outflow: observations and implications for numerical models, J. Geophys. Res., DOI: 10.1029/2012JA017975 , 2013 .

Nilsson,N., I. A. Barghouthi, R. Slapak, A. I. Eriksson, and M. André ,Hot and cold ion outflow: Spatial distribution of ion heating, J. Geophys. Res., 117, A11201, Doi: 10.1029/2012JA017974, 2012.

Nilsson. H., Waara,M., Arvelius, S., Marghitu,O., Bouhram, M., Hobara, Y., Yamauchi, M., Lundin,R., Rème,H., Sauvaud, J.-A. , Dandouras,I., Balogh, A., Kistler,L. M.,Klecker, B., Carlson. W., Bavassano-Cattaneo,M. B., and Korth,A.; Characteristics of high altitude oxygen ion energization and outflow as observed by Cluster; a statistical study, Ann. Geophys., 24, 1099-1112, 2006.

Retterer, J. M., Chang, T., Crew, G. B., Jasperse, J. R., and Winningham, J. D.: Monte Carlo modeling of oxygen ion conic acceleration by cyclotron resonance, Phys. Rev. Lett., 59, 148–151,1987a.

Retterer, J. M., T. Chang, G. B. Crew, J. R. Jasperse, and J. D. Winningham, Monte Carlo modeling of ionospheric oxygen acceleration by cyclotron resonance with broad-band electromagnetic turbulence, Phys.Rev. Lett., 59, 148–151, doi:10.1103/PhysRevLett.59.148 , 2004.

.Retterer, J. M., T. Chang, G. B., Crew, J. R. Jasperse, and J. D. Winningham, Monte Carlo modeling of oxygen ion conic acceleration by cyclotron resonance with broad-band electromagmetic turbulence, in physics of space plasma, SPI Conf. Proc. And Reprint Ser.,No. 6,edited by T. Chang , J. Belcher, J. R. Jasperse, and G. Crew, pp.97-111, Scientific, Cambridge, Mass., 1987b.

Retterer, J.M., Chang, T., Jasperse, J.T. Transversely accelerated ions in the topside ionosphere. Journal of Geophysical Research 99, 13,189–13,201, 1994.

Schunk, R. W. and A. F. Nagy, Ionospheres: physics plasma physics, and chemistry, Cambridge, 2000.

Schunk, R. W., Mathematical structure of transport equations for multispecies flows, Rev. Geophys., 15, 429, 1977.

Smith ,M.F.,and lockwood, Earths magnetospheric cusps , Rev. Geophys,34 , 233- 260,1996.
Takisuka, T., and H. Abe, A binary collision model for plasma simulation with a particle code, J. Comput. Phys., 25, 205, 1977.

Tam, S.W.Y., Chang, T., Pierrard, V.: Kinetic modeling of the polar wind, Journal of atmospheric and solar-terrestrial physics, 69, 1984 – 2027, 2007.

Tsurutani,B.T.andG.S.Lakhina,Some Concepts of wave-particle interaction in the Collision less plasmas,Reviews of Geophysics ,35,4,491,1997.

Winkler, E., J. P. St.-Maurice, and A. R. Barakat, Results fromimproved Monte Carlo calculations of auroral ion velocity distributions, J. Geophys. Res., 97, 8399– 8423,1992.

Winningham, J. D., and Burch, J.: Observations of large-scale ion conic generation with DE-1, Physics of Space Plasmas, 5, 137-158, 1984.

Yau, A. W., T. Abe, and W. K. Peterson, The Polar Wind: Recent Observations, J. Geophys. Res., 90, 8417, 1985, 2007.

http://www.nasa.gov

http://www.miniphysics.com

http://en.wikipedia.org/wiki/Magnetosphere

http://ssdoo.gsfc.nasa.gove

https://www.google.ps/search

Appendices

Appendix A: Monte Carlo simulation

(A.1) Generation of ions Velocity:

The starting point in the plasma simulation is the injection of an ion into the simulation region , and chosen it with a random initial velocity that corresponds to the distribution function of the ion at the injection point , but at the top of the par sphere (just below the exobase)The ion velocity distribution function was assumed to be non-drifting maxwellain , which can be written as :[Barghouthi et at ; 2003 a, b]

$$f(v) = n[\frac{m}{2\pi kT}]^{\frac{3}{2}} e^{\frac{-mv^2}{2kT}} \quad \dots\dots\dots\dots\dots\dots\dots\dots (A.1)$$

Where, k is Boltzmann's constant, T is the temperature at the injection point (i .e from boundary condition) , n is the number density ,m is the mass of the ion, and is the random velocity of the injected ion.

The ion velocity vector can be analyzed in two components , with respect to the direction of the magnetic field (B_0) the two components are :- Parallel to B_0 , which represented by V‖and the perpendicular toB_0, which represented by V⊥ , so it is recommended to represent the square of the velocity as :

$v = v_{\|} + v_{\perp}$'there we can rewrite Equation (A.1) as:-

$$f(v) = n[\frac{m}{2\pi kT}]^{\frac{3}{2}} e^{\frac{-m({v_{\|}}^2+{v_{\perp}}^2)}{2kT}} \quad \dots\dots\dots\dots\dots\dots (A.2)$$

This can be written as:

$$f(v) = n\left[(\frac{m}{2\pi kT})^{\frac{1}{2}} e^{\frac{-m{v_{\|}}^2}{2kT}} \right] \left[\left(\frac{m}{2\pi kT}\right) e^{\frac{-m{v_{\perp}}^2}{2kT}} \right]$$

$$= nf(v_{\|}) f(v_{\perp}) \dots\dots\dots\dots\dots\dots\dots\dots (A.3)$$

with

$$f(v_{\perp}) = \left[\left(\frac{m}{2\pi kT}\right) e^{\frac{-mv_{\perp}{}^2}{2kT}}\right] \ldots\ldots\ldots\ldots\ldots\ldots (A.4)$$

$$f(v_{\parallel}) = n\left[\left(\frac{m}{2\pi kT}\right)^{\frac{1}{2}} e^{\frac{-mv_{\parallel}{}^2}{2kT}}\right] \ldots\ldots\ldots\ldots\ldots\ldots\ldots\ldots (A.5)$$

Where $f(v_{\perp})$ is the injected ion velocity distribution function which perpendicular to the geomagnetic field lines and $f(v_{\parallel})$ is the injected ion velocity distribution function paralled to the geomagnetic field lines , we will use them to generate parallel velocities ($v_{\parallel s}$) and perpendicular velocities($v_{\perp s}$) of the injected species

(A.2) Generation of $(v_{\perp s})$:

[Aldrich . 1985]We want to get the values for random variable of ions perpendicular velocity $(v_{\perp s})$ at the starting point" injection point "which is distributed over the interval (0.∞) , with probalbility density equal to one which given by :

$$p(v_{\perp s}) = 2\pi\, v_{\perp s}\, f(v_{\perp s}) \ldots\ldots\ldots\ldots\ldots\ldots\ldots\ldots (A.6)$$

But if we substitute equation (A.2) into equation (A.5) , we can get the values of $v_{\perp s}$ are given by: Where$\grave{G}$ is arandom number which taken values between (0,1) , the value of ions perpendicular velocity($v_{\perp s}$)can be obtained solving equation (A.6) or (A.7)

$$v_{\perp s}^2 = -\left(\frac{2KT_s}{m_s}\right) In\left(1-\grave{G}\right) \ldots\ldots\ldots\ldots\ldots\ldots\ldots\ldots (A.8)$$

The means an ion is injected or initiated with a random ions perpendicular velocity ($v_{\perp s}$) at the starting point or the exobase

(A.3) Generation of ($v_{\perp s}$):

We must investigate between the local number of ions with $v_{\parallel s}$ and the actual number of those ions , with can passed through the lower boundary of the simulation region , which in the polar wind region is a geomagnetic tube extending from r=1.7 R_E to r = 13.7 R_E

We chose it (i.e. those ions $v_{\parallel s}$<0 will not passed through thro through the assumed injected boundary).

The probability of finding an ion pass through the lower boundary (injection point) is proportional to the ion flux (i.e. is the probability of these ions with $v_{\|s}$>0.

Were they can reach and cross the lower boundary) , which is given by :-

$P(v_{\|s})= P(v\|s)_{local} \times \alpha$ ……..…….. (A.9)

where

$$p\left(v_{\|s_{local}}\right) = f\left(v_{\|s}\right) = \left[\left(\frac{m_s}{2\pi k T_s}\right)^{\frac{1}{2}} e^{\frac{-m_s {v_{\|s}}^2}{2kT_s}} \right] \dots\dots\dots\dots\dots\dots\dots\dots (A.10)$$

This is given from equation (4) and α is normalizing constant

$$(i, e \int_0^{\infty} p\left(v_{\|s}\right) dv_{\|s} = 1)$$

We obtain the formulation that represents the probability density as:-

$$p\left(v_{\|s}\right) = 2\pi v_{\|s} \left[\left(\frac{m_s}{2\pi k T_s}\right) e^{\frac{-m_s {v_{\|s}}^2}{2kT_s}} \right] \dots\dots\dots\dots\dots\dots\dots\dots\dots\dots (A.11)$$

The value of ions parallel velocity$\left(v_{\|s}\right)$ can be obtained by solving the above equation (i, e equation (A.10), same as we solved equation (A.6) , which is equal to :-

$$v_{\|s}^2 = -\left(\frac{2KT_s}{m_s}\right) In\left(1 - \grave{G}\right) \dots\dots\dots (A.12)$$

We want to draw the attention that the formulas for$v_{\perp s}$ and$v_{\|s}$ are similar, but they have different numerical value due to$\grave{G}$, here we randomly generated an ion from maxwellian distribution ar the boundary level.

(A.4) The Distribution Function:-

We discussed in the previous sections that we need in simulation process to inject 10^6 ions from the injecting point $r = 5{,}9RE$ the injecting point (exbase).

These ions will be monitored until they escape from the chosen simulation region ,which extends from $r_0 = 5{,}6\ Re\ \ to\ r = 16Re$,At each altitude in the simulation region the

behavior Of these ions were monitored by a two dimensional grid in the velocity space $(v_{\|s}, v_{\perp s})$,so as to calculate the distribution function.

The velocities of the tested ions that they cross one of the monitoring altitude, we can be used to calculate the moments of the distribution function at that altitude.

The time that an ion spend in each bin divide by the bins volume is taken to be proportional to the ion velocity distribution function at the center of that bin [Barghouthi etal .2003a] ,But we use the symmetry in azimuthal direction to simplify the registration process, therefore the volume of the bin in velocity space can be represented as and$\Delta v^3 = 2\pi \Delta v_{\perp} \Delta v_{\|}$ and $f(v) d^3 y$ is equl to the number of the ions with velocities between v and $v + dv$,there for the time needed for the ion to pass through that bin is :-

$$\mathrm{t} = \frac{c_1}{|v_{\|s}|} \ldots\ldots\ldots\ldots \quad \ldots\ldots\ldots (A.13)$$

Where, c_1 is chosen to be arbitrary constant and it represents the width of the bin, but

$$fs(v) \ \alpha \ \frac{\frac{c_1}{|v_{\|s}|}}{2\pi \ v_{\perp s} \Delta v_{\|s} \Delta v_{\perp s}}$$

$$So \ \ fs(v) = \frac{\frac{c2}{|v_{\|s}|}}{2\pi \ v_{\perp s} \Delta v_{\|s} \Delta v_{\perp s}} \ldots\ldots\ldots (A.14)$$

Let the width of the bin sides equals to $\frac{1}{3}\left(\frac{2KTt}{m_t}\right)^{1/2}$ which is (1/3 of the thermal speed of the background ions)

So,

$$\Delta v_{\|s} = \ \Delta \ v_{\perp s} = \ \frac{1}{3}\left(\frac{2KT_t}{m_t}\right)^{\frac{1}{2}} \ldots\ldots\ldots\ldots\ldots\ldots\ldots (A.15)$$

Must keep in mind that the volume of each bin does not change , but these bins different volume , the makes that the distribution function to be written as:-

$$f_s(v) = \ \frac{c}{|v_{\|}|} \ldots\ldots\ldots\ldots\ldots\ldots (A.16)$$

Where c is an arbitrary constant

At each predetermined, so by knowing the parallel $V_{\|}$and the perpendiculare $V_{\perp}$velocities of that ion we can determine the location of the tested ion.

We use two integers such as J and I to determine the location of the ion where $J = INT\ (3\ V_{\perp_S})$ and we taka in consideration that ion parallel velocity ($V_{\|_S}$) is symmetric around the ion perpenelicular velocity ($V_{\perp_S}$) .

So J takes the integers from o to 10 , the greatest value for J was chosen to be 10, because it corresponds to a velocity three times higher than the thermal velocity of the background ions, which is difficult for the tested ion to reach.

Therefore, we put insert aretraction J such that $J = M_{in}\ (J, 10)$ to make sure that sorting is inside the array on the other hand, we get the parallel direction (i,e the value of I) byconsidering the boundaries of the bins at $((-9{,}5 - 8{,}5 \ldots .8{,}5\ \ 9{,}5)$

Since there is no azimuthal symmetry, where the value of I can be calculated by

$I = NINT\big(3 \times V_{\|_S}\big)$,which take the values between (-10,10) every bin will be known by (I, J) and altitude), therefore if the ion crossed a certain bin we can put the numerical value of $(f_{\ S}V_S)$ in that bin, after that if another ion crossed the same bin we add its numerical value of $(f_{\ S}(V_S)$ to the previous one. we kept doing the above procedure until we finished all the ions, so after running the model we get the numerical values for all bins, there for we get the graph for the distribution function of the ions at each altitude by connecting between the bins that of$(f_{\ S}(V_S)$,[Barghouthi et al ,2003]

(A.5) Moments of the distribution function:-

We seek to obtained the moments of the ion (i,e. density ɳ ; drift velocity u, parallel temperature$T_{\|}$, and perpendiuclare temperatur$T_{\perp}$, at each altitude. The ions distribution function f_s (V_s) is can be written as:-

$$f(v_s) = qc_2 \sum_i \frac{1}{\left|(v^i_{\|_S}\right|} \frac{\delta\left(V_{\|_S} - {V_{\|_S}}^i\right) s\ (\ V_{\perp_S} - {V_{\perp_S}}^i)}{2\pi {V_{\perp_S}}^i} \ldots\ldots\ldots\ldots . (A.17)$$

Where δ(x) is the Dirac delta function

[Barak at and Schunk 1982 c],the superscript I denotes that the summation is over all continuous segments of the monitored ion trajectory in the velocity.

We used the above distribution function to find the expression for the moments in the following subsections

(A.5.1) The Density:-

The number density of ions can be written as:-

$$n_s \int f_s\,(v_s) dv_s^3 = 2\pi \int f_s\,(v_s)\; dv_{\|s} v_{\perp s} d\; v_{\perp s} \dots\dots\dots\dots\dots\dots\dots (A.18)$$

$$= q\; c_2 \sum_i 2\pi \int \frac{\delta\left(V_{\perp s} - {V_{\perp s}}^i\right)\delta\left(V_{\|s} - {V_{\|s}}^i\right) dV_{\|s} V_{\perp s}\, dv_{\perp s}}{2\,\pi\,\left|V_{\|s}^i\right| V_{\perp s}^i}$$

$$n_i = q\; c_2 \sum \frac{1}{\left|V_{\|s}^i\right|} \dots\dots\dots\dots\dots\dots\dots\dots\dots (A.19)$$

Therefore , after calculating the location of the test ion (i.e the bin) we add the density store $\frac{1}{\left|V_{\|s}^i\right|}$

(A.5.2) The drift velocity:-

The drift velocity u of test ions s is equal to of the expectation value of $V_{\|s}$(i.e<$V\|_s$>):-

$$u_s = \frac{\int v_{\|s} f_s(v_s) d^3 v_s}{\int f_s(v_s)\; d^3 v_s}$$

$$= \frac{\int \mathrm{d}v_{\|s} v_{\perp s} dv_{\perp s}{}^3\; 2\pi \quad \sum_i \frac{\delta\left(V_{\perp s} - {V_{\perp s}}^i\right)\delta\left(V_{\|s} - {V_{\|s}}^i\right)}{2\,\pi\,\left|V_{\|s}^i\right| V_{\perp s}^i}}{\int \mathrm{d}v_{\|s} v_{\perp s} dv_{\perp s}{}^3 \quad 2\pi \sum_i \frac{\delta\left(V_{\perp s} - {V_{\perp s}}^i\right)\delta\left(V_{\|s} - {V_{\|s}}^i\right)}{2\,\pi\,\left|V_{\|s}^i\right| V_{\perp s}^i}} \dots\dots\dots (A.20)$$

$$u_{s=} \frac{\sum_i \frac{{V_{\|s}}^i}{\left|V_{\|s}^i\right|}}{\sum_i \frac{1}{\left|V_{\|s}^i\right|}} = \frac{\sum_i sign\;\left({V_{\|s}}^i\right)}{\sum_i \frac{1}{\left|V_{\|}^i\right|}} \dots\dots\dots\dots (A.21)$$

Where sign means (+) or (-)

(A.5.3) The perpendicular Temperature :-

The random thermal velocity is defined as $c_s = v_s - u_s$. from the expectation value of the kinetic energy ($\frac{1}{2}mc_s^2$).we can obtained the thermal energy ($\frac{3}{2}\ kT_s$), which is given by

$$\frac{3}{2}KT_s = \frac{\frac{1}{2}m_s[(V_{\|s} - u_s)^2 + V_{\perp s}{}^2]\int f_s(v_s)d^3v_s}{\int f_s(v_s)d^3v_s} \dots\dots\dots\dots (A.22)$$

$$\frac{1}{2}KT_{\|s} + KT_{\perp s} =$$

$$= \frac{\frac{1}{2}m_s[(V_{\|s} - u_s)^2 + V_{\perp s}{}^2]\int f_s(v_s)d^3v_s}{\int f_s(v_s)d^3v_s} + \frac{\frac{1}{2}m_s v_{\perp s}^2 f_s(v_s)\, d^3v_s}{\int f_s(v_s)d^3v_s} \dots\dots\dots\dots (A.23)$$

The perpendicular temperature is given by the expectation value of$T_{\perp s} = \frac{1}{k}\left(\left(\frac{1}{2}m_s V_{\perp s}{}^2\right)\right)$, which is the second term of the above equation,therefor $T_{\perp s}$ can be represented by :-

$$T_{\perp s} = \frac{m_s}{2K}\frac{\sum_i\left(V_{\perp s}{}^2\right)/\left|V_{\|s}^2\right|}{\sum 1/\left|V_{\|s}^2\right|} \dots\dots\dots (A.24)$$

(A.5.4) The parallel temperature :-

From equation (A.22), the parallel temperature is defined as :-

$$T_{\|s} = \frac{\frac{m_s}{K}\int(v_{\|s} - u_s)^2(\ v_s)\ d^3v_s}{\int f_s(v_s)d^3v_s}$$

$$T_{\|s} = \frac{\frac{m_s}{K}[v_{\|s} f_s(v_s)d^3v_s - 2u_s\int v_{\|s} f_s(v_s)d^3v_s + u_s^2}{\int f_s(v_s)d^3v_s}$$

And so , it is can be written as :-

$$T_{1\,1s} = \frac{m_s}{K}\left[\frac{\sum_i\frac{(v_{\|s}^i)^2}{v_{\|s}^i}}{\sum_i\frac{1}{\left|v_{\|s}^i\right|}} - \left[\frac{\sum_i sign\left(V_{\|s}{}^i\right)}{\sum_i\frac{1}{\left|v_{\|s}^i\right|}}\right]^2\right] \dots\dots\dots\dots (A.25)$$

Where sing means (+) or (-).

Therefore, we found the solution of Boltzmann equation i.e. the distribution function $f_s(V_s)$ and the moment of the distribution function by using the Monte Carlo simulation.

الملخص

واحدة من نتائج التفاعلات الأرضية الشمسية الأكثر أهمية هو تدفق الأيونات على علو عالي، إن عملية تزويد ايونات الهيدروجين وأيونات الأكسجين بالطاقة الناتجة عن تفاعل هذه الأيونات مع الاضطراب الكهرومغناطيسي لها تأثير مباشر على انتشار هذه الأيونات في المنطقتين (cusp, central polar cap).

لقد تم التحقق من عملية تأثير التفاعل بين هذه الأيونات مع الأمواج الكهرومغناطيسية والتي بدورها تؤثر على توزيع أيونات فضاء السرعة وكذلك على وضع الارتفاع باستخدام محاكاة مونتي كارلو.

وهذه الطريقة تتضمن تأثير كل من (مجال الجاذبية ، المجال الالكتروستاتيكي المستقطب ، المجال المغناطيسي الأرضي)، هذا بالإضافة الى تأثير تفاعل الأيونات مع الأمواج الكهرومغناطيسية في منطقة المحاكاة والتي تمتد من (1.7 -14.9) انصاف اقطار نصف قطر الأرض .

إن تأثير الارتفاع وكذلك فضاء السرعة على التفاعل الحاصل بين الأيونات مع الأمواج الكهرو مغناطيسه ثم إدراجه بتعديل فضاء السرعة بزياده أخذت عشوائيا بمقدار صغير هو ($\Delta V_\perp$) وفقا ل($(\Delta V_\perp)^2 = 4D_\perp \Delta t$) حيث $D_\perp$ هو معامل الانبثاق وΔt هو التغير في الزمن.

كانت نتيجة الدراسة كالأتي: في الفصل الثالث، استخدمنا معامل نيلسون وآخرون (2013) التي تم حسابه من خلال المركبة الفضائية (Cluster) للحصول على السلوك مع الارتفاع لأيونات O^+ , H^+ . وفي الفصل الرابع قمنا بالمقارنة بين هذه النتائج المحاكاة و نتائج المحاكاة التي تم الحصول عليها باستخدام معامل الانتشار للبرغوثي (1997) و(1998) الذي تم الحصول عليه من المركبة الفضائية (Dynamics Explorer spacecraft).

تم عمل مقارنة لمنطقتي (central polar cap and cusp regions) بين معامل الانبثاق ل (Barghouthi) و(Nilsson). ومن الواضح جدا أن هناك فرقا كبيرا بين كل من نتائج المحاكاة بسبب معاملات نشر مختلفة؛ ويعزى هذا الاختلاف إلى سلوك معامل الانتشار ومدار المركبة الفضائية. يمكن أن نقول أن القيم العددية بسبب (DE-1satellite)هي أعلى بكثير من القيم المناظرة بسبب(Cluster). ويرجع سبب الاختلاف الى مدار القمر الصناعي، والظروف الجيوفيزيائية المختلفة.